Comparing heart assist devices, using a lumped parameter model and mock-loop

van de Meerakker, T.

Award date:
2020

Master's Thesis

Comparing Heart Assist Devices, Using a Lumped Parameter Model and Mock-Loop

Author:
T. van de Meerakker
0865482

Graduation committee:
Prof. dr. ir. F. van de Vosse
Dr. ir. M. Rutten
D. van Dort, MD
Dr. ir. J. Foolen
K. Peij, BSc

8ZM200
Group of Cardiovascular Biomechanics
Department of Biomedical Engineering

December 11, 2019

Abstract

Introduction: A last-resort treatment option for cardiogenic shock (CS) is mechanical circulatory support (MCS). MCS has existed for over five decades and has therefore led to development of several MCS devices. Four examples of these devices are the intra arterial balloon pump (IABP), the Impella 2.5, the PulseCath iVAC 3l and the TandemHeart. Each of these devices give support in a different way, leading to support of the cardiovascular system in different ways.

In order to compare different MCS devices, in vivo animal tests studies are normally used. Animal tests may give a good indication of MCS performance in patients, but differences between human and animal anatomy can cause differences in results. Furthermore, results of these animal tests are also subject to variance, since bodies are never truly identical. Alternative testing methods may therefore be preferred.

Two alternative testing methods are simulation tests, based on lumped parameter models and experimental set-ups known as mock-loops. This study attempted to compare the mentioned MCS devices, using both of these different test methods.

Methods: The Lumped Parameter model that was used, was based on the work by *Schampaert et al. (2011)*. This work also used the implemented IABP simulation with 1:1 support ratio. The Impella 2.5 was implemented by draw of volume from the left ventricle (LV) into the aorta. Flow through the Impella was made pressure-dependent derived from flow profiles from similar pumps. The TandemHeart had draw from the left atrium (LA) and outflow into the femoral artery, also with pressure-dependent flow. The PulseCath had draw from the LV into the aorta with a prescribed pulsatile flow profile.

The mock-loop at the Eindhoven University of Technology was used for the mock-loop experiment. MCS devices were connected to the set-up as they were implemented in the lumped parameter model, except for the TandemHeart outflow catheter, which was connected to a distal part of the aorta.

Results: The lumped parameter model and mock-loop model show differences per MCS device, regarding flows and pressure values. Each device therefore has a different impact on both the perfusion of the cardiovascular system and the unloading of the LV. Different results between these two models exist.

Discussion: The results of both methods have been evaluated. The lumped parameter model showed results that were more according to literature than the mock-loop model. The physical limitations are the cause of this problem. The devices simulated in the lumped parameter model may be comparable to literature, but flow data is not based on direct measurements.

Conclusion: The evaluated MCS devices either increase cardiovascular perfusion, cause ventricular unloading or both, depending on the device and testing method. Furthermore, the two testing methods may both be acceptable methods to test prototype MCS devices, but improvements need to be implemented in both cases, in order to draw reliable conclusions.

Contents

Chapter 1

Introduction

1.1 Introduction

Over the last years, life expectancy has risen in Europe. According to the World Health Organization, the life expectancy of the average European was 77.5 years in 2016, whereas this was 75.7 years in 2010 [1]. Though a rising life expectancy is an improvement, life threatening diseases will always exist. The clear number one cause-of-death disease in high-income countries is ischaemic heart disease, with over 140 reported deaths per 100,000 population [2]. This gives reason to investigate treatment options for these kind of diseases, for example dilated cardiomyopathy (DCM).

A last-resort treatment for DCM is heart transplant. However, people that are suffering from DCM cannot easily get a heart transplant, due to an insufficient number of available donor hearts [3]. This results in a higher average waiting time for heart transplant, which is over two years today [4]. Logically, this can lead to hemodynamic deterioration for some of these patients.

Another example for which heart transplant is used as a last-resort treatment option, is cardiogenic shock (CS). CS may follow from acute myocardial infarction (MI) [5]. Patients suffering from CS have end-organ hyppoperfusion and hypoxia which can be life threatening [6]. For the same reasons as for DCM patients, CS patients cannot always be treated with heart transplant.

CS therefore needs alternative treatment options. The so-called *"Should We Emergently Revascularize Occluded Coronaries for Cardiogenic Shock"* (SHOCK) trial has shown that early reperfusion of the infarct related artery by percutaneous coronary intervention (PCI) gives a significant survival benefit, compared to initial stabilisation with pharmacological support [7]. Therefore, PCI is now an accepted therapy.

Despite early revascularisation by PCI, mortality of cardiogenic shock remains twice as high, compared to a combination of PCI and Intra-aortic balloon counterpulsation (IABC) after a period of six months [8]. IABC is one of the treatment options, which uses a mechanical circulatory support (MCS). MCS devices are able to support the heart mechanically. MCS devices are increasingly important for the clinical world and have therefore undergone substantial progress in development [9]. Some of the milestones of these developments are discussed in the next paragraph.

1.2 Heart Transplants and Mechanical Circulatory Support: A Brief History

The concept of MCS has existed for decades. The first clinical use of a left ventricular assist device (LVAD) was in 1963 [10] in the USA. The patient who received this LVAD, underwent a prosthetic valve replacement. Complications of this procedure, led to severe brain damage and pulmonary edema. The edema was successfully cleared by implanting the LVAD. Though the patient that underwent the surgery died, usage of MCS continued. In 1966, another patient underwent MCS since newly transplanted valves could not be weaned. After ten days of VAD support, patient recovery was a fact, making this procedure the world's first successful VAD procedure [10]. This was one year before the first successful human-to-human heart transplantation was performed in South-Africa [11]. While a first complete heart transplant is considered a bigger milestone than the first successful MCS procedure, it is worth noting that these events occurred at approximately the same time, meaning that development of both procedures happened simultaneously.

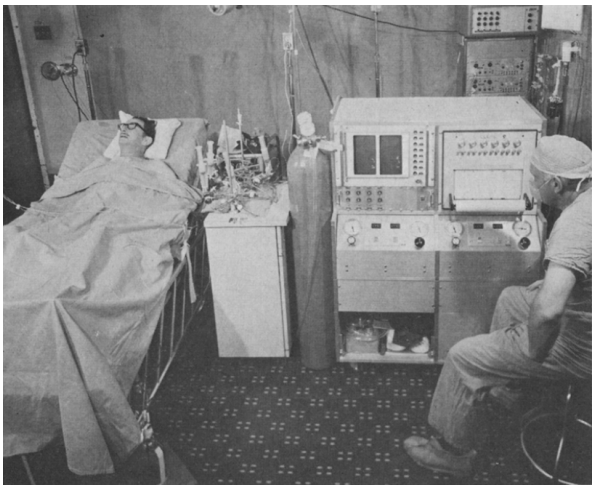

Figure 1.1: Set-up in the equipment in the IC, as was done by *Cooley et al. (1969)*

In the early 60's, before these previous milestones occurred, the Artificial Heart Program in West-Berlin started. As the name suggests, the goal of this project was to develop a total artificial heart (TAH). It also researched natural-artificial material interactions, fatigue testing and, of course, pump development. This project took several decades of time and had several complications. A status report of 1985 discussed material failure and pump malfunction among other problems [13]. Although these issues existed, MCS was still used as a bridge-to-transplantation (BTT), with the first implantation of the TAH in 1969 [14]. While the TAHs of this time were less developed than current TAHs, the computer technology that was used to control these devices was also completely different from today's standards. Figure 1.1 shows a set-up as used by *Cooley et al. (1969)* [15]

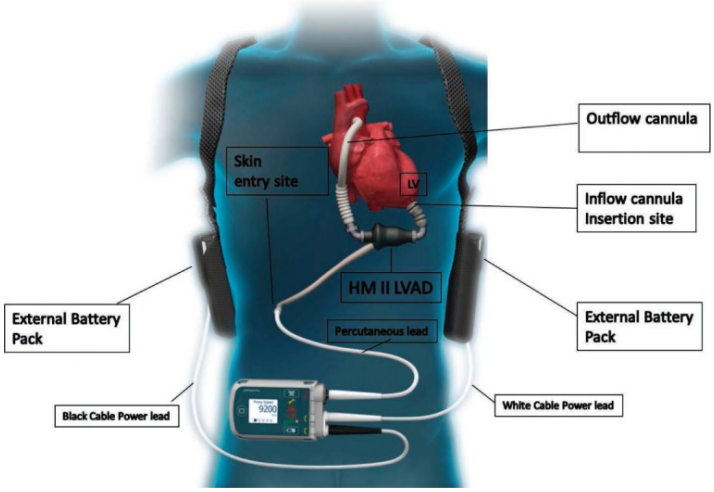

Figure 1.2: Schematic view of an implanted HeartMate II and equipment. (Image taken from *Estep et al. (2015)* [12])

During the 1980's, the number of heart transplants increased exponentially. According to *The International Society for Heart and Lung Transplantation Transplant Registry*, the number of heart transplants in registered centres went from approximately 200 in 1982 to almost 4000 in 1989, with a survival rate of 50% 8 years after transplantation [16]. During this time, procedures for MCS improved [17], leading to a low complication rate [18]. However, long-term use of these first-generation MCS devices led to mechanical failure [9], meaning that MSC use could only be used as a temporary solution at this time.

Development continued in the 1990's. The HeartMate II LVAD, at that point still known as the Nimbus, was one of the devices that led to a better BTT, partly because of its low failure rate, compared to earlier devices [19]. This was made possible with impellers, since usage of impellers allowed for a smaller and more stable design of devices. A schematic view of the HeartMate II can be found in figure 1.2. The HeartMate II is not the only device of the second generation that uses an impeller. In 1992, *Sasaki et al. (1992)* published their article, reviewing the second-generation cardiopulmonary bypass system, which also made use of an impeller, allowing the device to be compact [20]. Although the size of the second-generation LVADs improved, survival rates were still considered low: *McBride et al. (1999)* evaluated the Thoratec VAD and stated that VAD support still remained associated with a significant morbidity in 1999 [21]. This meant that destination therapy for MCS, though possible, was not recommended.

MCS implantation took a big leap around the year 2000 again. Of the patients who received transplant during the year 1999, 15% were on MCS. This number rose to 27% in the year 2001 [22]. The *REMATCH trial* evaluated the long term use of LVAD support (specifically the HeartMate vented electric device) and found that LVADs can be acceptable alternatives for patient who are not eligible for heart transplantation [23]. In the year 2002, the American Food and Drug Administration (FDA) approved the MCS program as destination therapy [4]. Approval of destination therapy of MCS meant that MCS became an actual alternative for heart transplantation, which is clearly a significant milestone. The outcomes of destination therapy in the so-called post-REMATCH era, were described in 2007 and showed that patients had an excellent chance of 1-year survival if destination therapy was prescribed before major complications of heart failure had developed [24]. This showed that use of LVAD support was, from this moment on, a viable treatment option.

1.3 Different Types of Mechanical Assist Devices

With over five decades of research in MCS devices, it is only logical that numerous devices are being used in the clinical world today. Because of the different development of these devices, a difference in their implementation exists. Some of these devices can be implemented percutaneously, while others need to be implanted surgically. A few examples of MCS devices are described below, subdivided into these two categories.

1.3.1 Percutaneously Implanted Mechanical Circulatory Support Devices

One of the earlier mentioned devices is the Intra-aortic balloon pump (IABP). This device is inserted via the femoral artery into the descending aorta [25]. The balloon of the IABP is inflated during diastole and deflated during systole, meaning that the IABP uses counter pulsation, to increase blood flow through the arteries during the diastole. The inserted IABP is shown in figure 1.3 in both the systole and diastole.

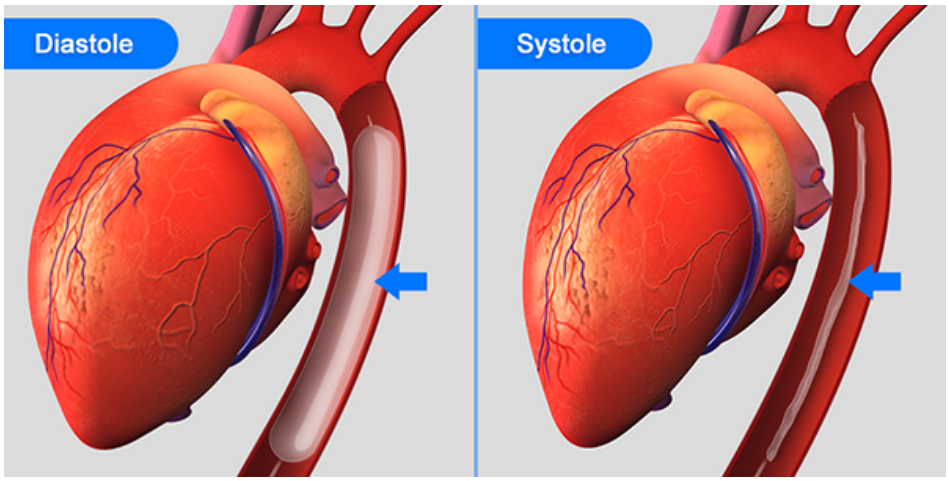

Figure 1.3: An inserted IABP in both systole and diastole. Image taken from NMC Heartcare [26].

The use of counter pulsation leads to a lower after-load during the systole, which in turn lowers the necessary work of the failing LV [27]. It also increases blood flow through the coronary arteries [28], which may increase oxygen uptake from the heart itself. The pulsation rate of the IABP is equal to that of the supported heart. Timing of the cycle phase of the IABP, relative to that of the heart, is the most important determinant of effective counter-pulsation. Other factors that include the effect of the IABP are the volume of the balloon, the position of the balloon in the aorta, the heart rate and -rhythm, the aortic compliance and the vascular resistance [29].

Another MCS device, which is also inserted via the femoral artery, is the Impella. Unlike the IABP, the Impella is a percutaneous LVAD (pLVAD) which is inserted through the aortic valve (AV) and pumps blood from the LV into the aorta, providing higher mean blood flow from the LV into the arteries. The Impella is inserted and held in place by a catheter. An inserted Impella device is schematically shown in figure 1.5.

Currently, there are multiple Impella devices on the market. The basic principle of these devices is the same, but these devices have a different flow rate, ranging from 2.5 l/min to 5 l/min [30]. Impella devices have a continuous flow during both the systole and diastole, making the regulation of flow through the Impella independent of heart rate.

By pumping blood, Impella devices support the heart by reducing the LV's required stroke volume (SV). Since the average blood flow through the AV is approximately 5 l/min, the required cardiac output done by the LV itself is negligible, when the Impella is able to create a flow of 5 l/min. However, performance of the LV is still present.

The Impella can be used as a BTT with a short-term use of no more than four days of mechanical support [31]. Impella utilisation is, however, not without risk, since it can for example damage the AV. Chances of this occurring are rare, however [32]. Another report discussed a clinical case, where the suction port struck the LV wall with a pendulum motion, but this is also a rare case [33]. Still, a recent study showed that use of the Impella comes with higher rates of bleeding and ischaemic complications, compared with the IABP and recommends more strict patient selection for the Impella [34].

Similar to the Impella are the PulseCath devices. These PulseCath devices are pLVADs,

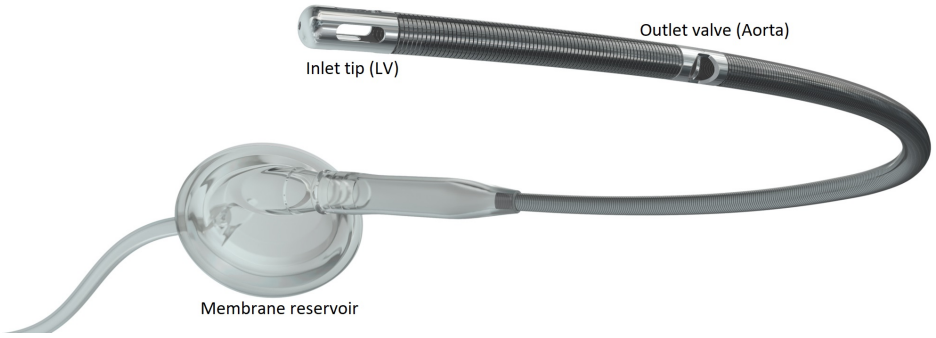

Figure 1.4: The PulseCath iVAC 3l. Image taken from *den Uil et al.* [35].

which are also inserted and held by a catheter. Like the Impella, these devices draw blood through the inlet in the LV and pump out blood through the output in the aorta [36]. However, blood flow through these devices is pulsatile instead of continuous. Pulsatile outflow to the aorta occurs during diastole, while the inflow occurs during systole [37]. Blood that is drawn from the LV, is stored in a 40 ml reservoir, which is extracorporeal. The PulseCath devices are controlled the IABP driver, which inflates and deflates this reservoir. The amount of maximum flow depends on the device. The PulseCath iVAC 3l can, for example, generate a maximum pulsatile flow of 3 l/min [38]. This model is shown in figure 1.4.

An alternative to the above discussed systems, is the TandemHeart, designed by TandemLife. This is a centrifugal pump, which is not implanted. The TandemHeart uses a transseptal cannula, which draws blood from the left atrium into this pump and a cannula which returns blood from the pump to the femoral artery, resulting in a complete bypass of the LV [39]. A schematic view of the transseptal cannula of the TandemHeart is shown in figure 1.6. Note that the TandemHeart passes through the atrial septum, into the RA, followed by the vena cava. The TandemHeart uses a centrifugal pump mechanism and delivers a maximum hemodynamic flow of 4 l/min [40]. This reduces the workload of the LV, by lowering the end-systolic pressure and end-diastolic volume. An overview of the bypass is shown in figure 1.7.

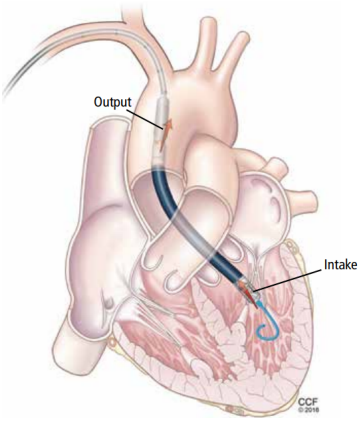

Figure 1.5: An inserted Impella device, with draw from the LV and output into the ascending aorta [41].

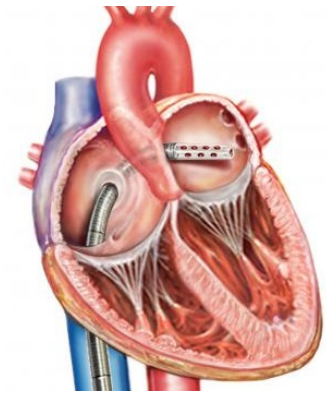

Figure 1.6: Schematic view of the TandemHeart transseptal cannula [42].

These devices are different in their design. An overview of the most important specifications of these four devices, is given in table 1.1 for comparison.

	IABP	Impella 2.5	PulseCath iVAC 3l	TandemHeart
Max. Flow (l/min)	N.A.	2.5	3	4
Pump type	IABP driver	axial	IABP driver	centrifugal
Position	Aorta	LV, aorta	LV, aorta	LA, RA, Vena Cava, femural artery
Operation type	Pulsatile	Continuous	Pulsatile	Continuous

Table 1.1: Main differences of the MCS devices as discussed above.

1.4 Validation of Mechanical Circulatory Support Devices

Logically, all MCS devices that are currently used in the clinic, went through thorough tests to determine performance and safety. One way to do this, is to do in vivo animal testing [44]. Animal tests may give a good indication of MCS performance in patients, but differences between human and animal anatomy can cause differences in results [45]. Results of these animal tests are also subject to variance, since bodies are never truly identical. Statistical variance could be lowered with a higher sample size, however, a higher sample size would have a negative effect on other concerns, e.g. ethical concerns, costs and time. Therefore, a preferable alternative might be a model, simulating the mechanical cardiovascular system.

Systems like these have already been used for multiple purposes, with every model different in its complexity and structure. A reason to use simulation systems for testing, is the consistency at which these systems work. This gives the possibility to study effects with the same system properties [46]. Modelled systems also give a better reproducibility, compared to animal testing, since device properties are known and measurements that would otherwise be too invasive, can be executed. A third advantage is the ability to compare the effects of

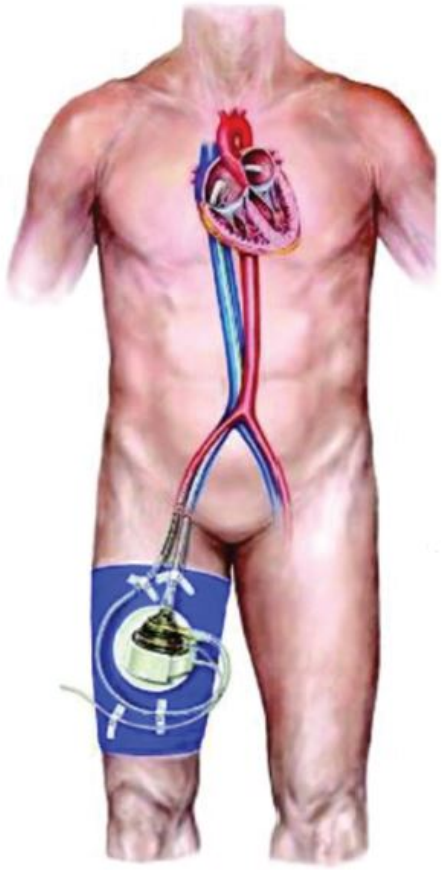

Figure 1.7: An overview of the bypass of the LV by the TandemHeart. Image taken from *Alabbady et al.* [43].

multiple changes and variances to the system, since all tests that are to be compared, can have the same baseline, which is in contrast with animal tests.

1.4.1 Lumped Parameter Models of the Circulatory System under Mechanical Circulatory Support

A lumped parameter model can describe the physiology of the circulation in terms of pressure-flow relations, using electric analogues for the blood vessels and heart chambers. Vessels are represented with RLC networks, describing the resistance, R, impedance, L and compliance, C. The heart chambers are represented by time-dependent compliances. The valves in the circulation are represented by diodes.

Bovendeerd et al. (2006) described the cardiovascular system based on this model structure, where the circulatory system consists of an LV, arterial system and peripheral system, as well as the coronary circulation [47]. This lumped parameter model subdivides the arterial system into RLC components, linked with nodes. Each node then represents a point of interest in the cardiovascular system. The model set-up is shown in figure 1.8. This model represents the parts of the circulatory system with nodes, where R_{art}, R_{per} and R_{ven} represent arterial, peripheral and venous resistance respectively. MV and AV represent the mitral valve and aortic valve, C_{art} and C_{ven} the arterial and venous compliances respectively and L_{ven} and L_{art} the venous and arterial inertia respectively. Pressures and flow are given by P_{art}, $P_{myo,c}$, $P_{ven,c}$, P_{ao} and P_{la}, the pressures in the arteries, myocardium, coronary veins, aorta and left atrium respectively, and q_{ao}, q_m, $q_{art,c}$, $q_{ven,c}$ the flow through the aortic valve, mitral valve, coronary arteries, and coronary veins respectively.

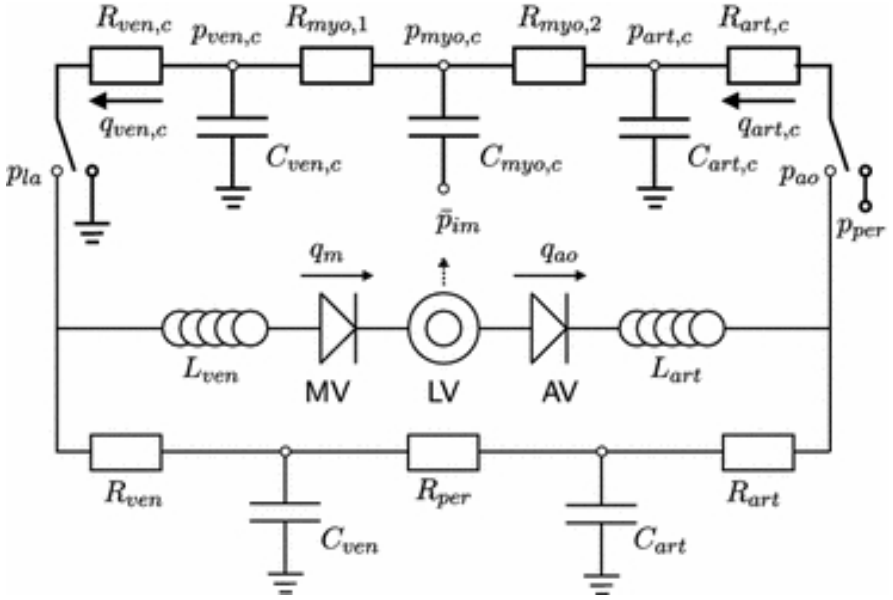

Figure 1.8: Lumped parameter model as used by *Bovendeerd et al. (2006)*

This model enables flow by changing the volume of the LV node, simulating systolic contraction. This enables flow through the AV. During simulation of the diastole, LV pressure drops. Since the AV is represented as a diode in the circulatory model, back-flow is not allowed, even when the LV pressure is lower than the arterial pressure. Blood flow will

occur, either through the coronary system, or the peripheral system, eventually leading the blood to the veins. Compliance of arteries and veins are represented by the capacitors in the system. Note that the extracellular pressure is represented by the ground in this electrical system. Since the modelled blood volume consists of significant mass, acceleration is a result of Newton's second law. This latency is represented by the inductances.

As said, this lumped parameter model may represent the circulatory system, but is, like all models, a simplified representation of reality. For instance, in this model, the entire arterial pressure is represented by only three nodes. This could still be a decent representation, when for example, general flow and pressure components are observed, but inadequate for observation of, for example, pressures in different parts of the peripheral and arterial system. In order to get realistic info for these parts, the model of *Bovendeerd et al. (2006)* needs additional segments.

Since the lumped parameter model is based on elementary nodes, it is relatively easy to add additional nodes, or to divide nodes into multiple nodes. *Schampaert et al. (2011)* added these additional nodes, in order to simulate blood flow through multiple nodal points. The set-up of this system is shown in figure 1.9. These additional nodes gave *Schampaert et al. (2011)* the possibility to study the effects of a simulated IABP in different sections of the aorta [48].

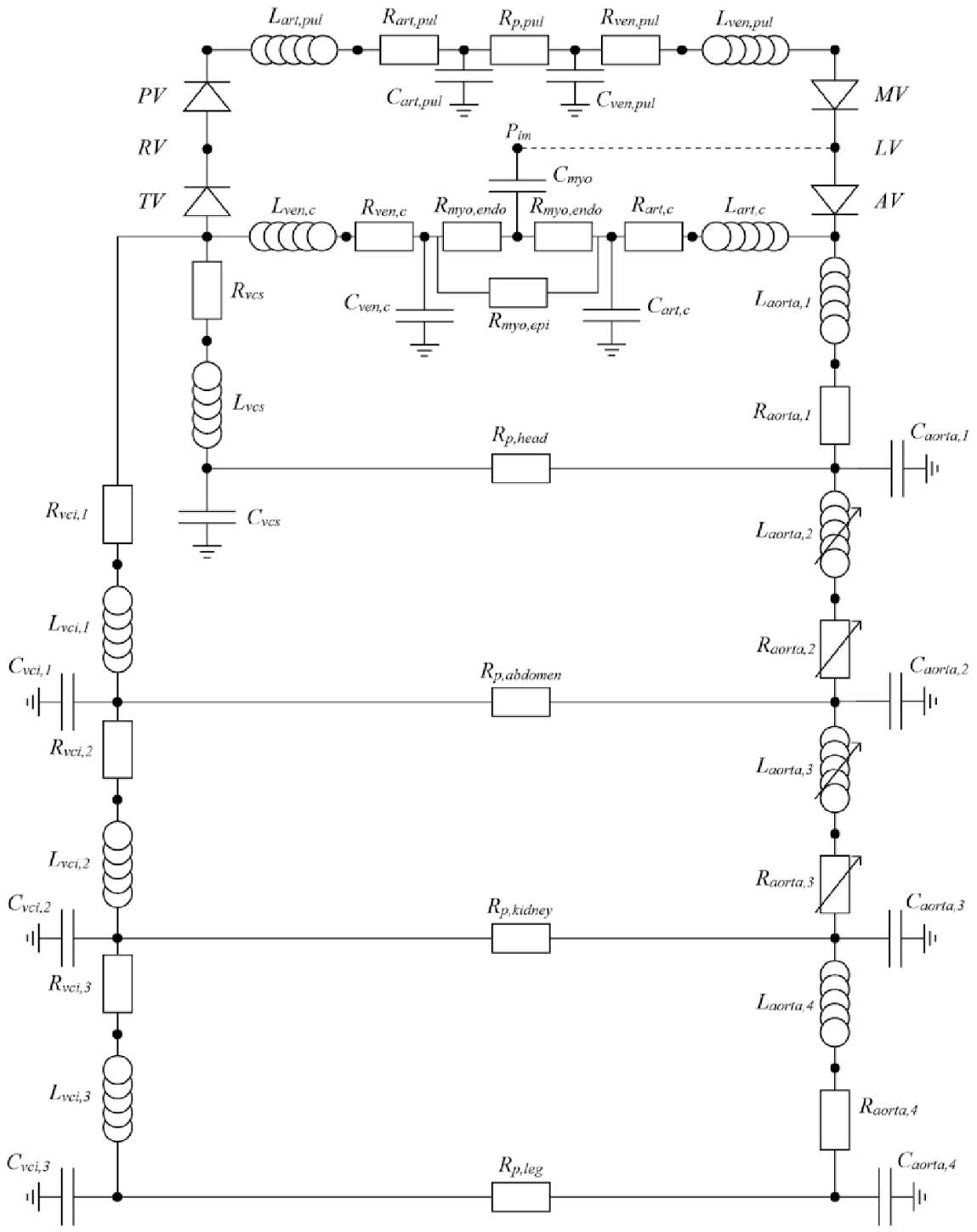

Figure 1.9: Set-up of the lumped parameter system as simulated by *Schampaert et al. (2011)*.

1.4.2 Circulatory lab model

The circulation is often modelled experimentally, in what is called a mock-loop. An example of such a mock-loop, is the mock-loop system at Eindhoven University of Technology (TU/e). The main components of the circulation are modelled as a series of tubes, tapered screws for resistance and compliance chambers.

In order to do this, two piston pumps are used to create fluid flow. Fluid in the LV is led into the aorta, made of silicone rubber for physiological compliance. From there, fluid flows into a three-element windkessel systemic afterload. From there, fluid is led into the right atrium (RA), followed by the right ventricle (RV). The motor of the RV pumps the fluid into the pulmonary artery, followed by the pulmonary afterload, again represented by a three-element windkessel model. Heart cycles are modelled by the Frank-Starling law, which make the cardiac output (CO) of the heart dependent on blood flow, for more realistic modelling behaviour.

A systematic overview of this system is shown in figure 1.10.

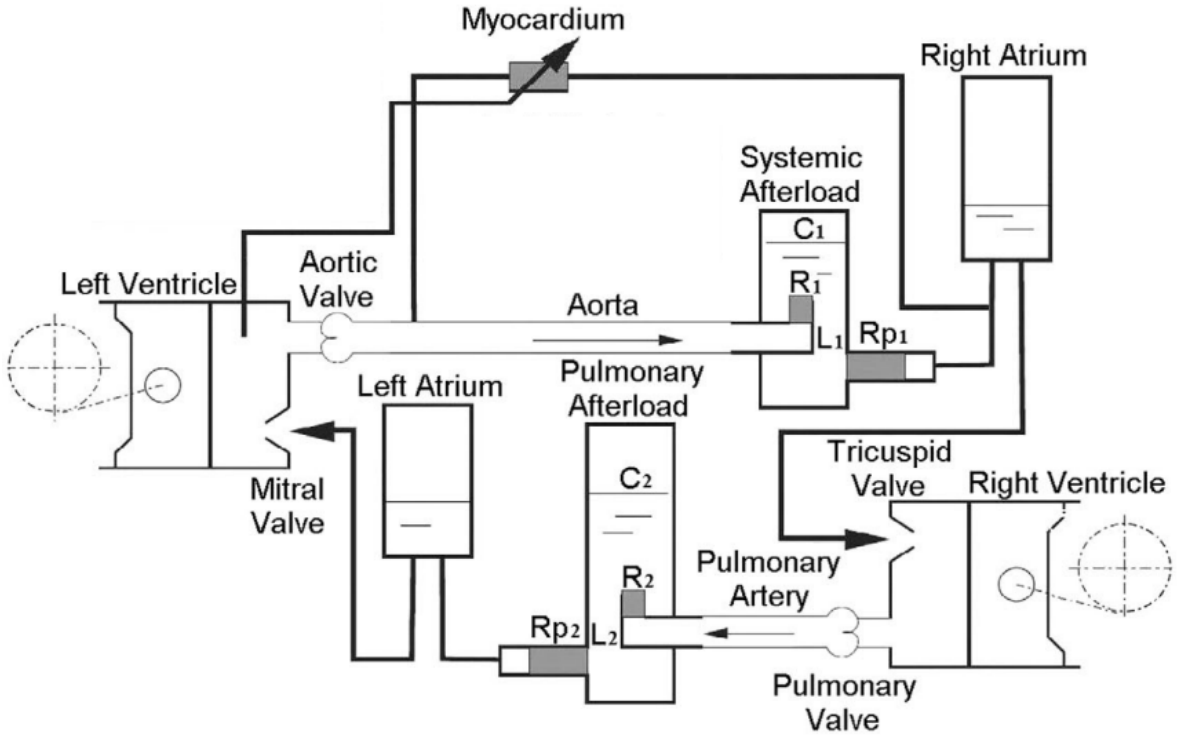

Figure 1.10: Schematic of the mock-loop system at TU/e [49].

1.5 Aim of this Study

Both the simulated lumped parameter models and the experimental mock-loop studies can be used to study clinically relevant properties of different MCS devices. Studying multiple devices would give a comparison of these devices, based on these relevant properties. This study will attempt to make a comparison of multiple MCS devices, using both the simulated lumped parameter model, and experimental set-up, as developed by *Schampaert et al. (2013)*.

To achieve this, properties of both models will be adjusted in order to model cardiac infarction, in order to form a baseline. This baseline will then be validated and adjusted until pressure and flow values of the system are, according to what literature describes as, criteria for cardiogenic shock. The MCS devices that will be compared in this study are the IABP, Impella 2.5, TandemHeart and PulseCath iVAC 3l.

Both experiments will be compared to each other and to literature values. Results between these two models should be comparable, if all cardiovascular properties and device properties are implemented correctly.

All devices will be evaluated, based on their influences on mean flow, arterial pressure, LV volumes and pressures and flow through MCS devices. It would be expected that MCS would improve mean flow and MAP, resulting in better perfusion. Secondly, the main function of MCS, mechanical unloading of the LV. It would therefore be expected that these MCS devices that will be used, would either cause the LV pressures to drop or lower SV. These effects will be evaluated for each simulation and validated with literature values.

Chapter 2

Materials and Methods

2.1 Simulation model

2.1.1 Model Specifications

Simulation of the cardiovascular system as a lumped parameter model was done with a Matlab model based on the model of *Schampaert et al. (2011)*. The set-up of the baseline, meaning a modelled patient without an implemented MCS device, is thus given in figure 1.9. The values of these systemic variables were kept as determined by *Schampaert et al. (2011)*, with the exception of heart valve resistance. The original value of $1 \frac{Pa \cdot s}{m^{-3}}$ caused high flow rates at low pressure gradients. Since MCS implementation caused oscillation, this gave unstable pressure and flow at the heart valves. The value of valve resistance was therefore set to $1 \cdot 10^6 \frac{Pa \cdot s}{m^{-3}}$, since this led to more stable calculations. All values are given in table 2.1. The MADs that were implemented in the simulation model were the IABP, Impella 2.5, PulseCath iVAC 3l and the TandemHeart.

Heart motion of this model was simulated with the one-fibre model, as was described by *Bovendeerd et al. (2006)* [47] based on the model by *Arts et al. (2003)* [50] This model represents all fibres, along with their orientation as a single fibre, wrapped around a core. This model describes heart contraction as one integral of the contraction of fibres in the entire ventricular wall. A representation of the model is shown in figure 2.1.

Inputs for this model are ventricle wall volume, ventricle cavity volume and fibre contractility, C, for active stress. In case of a healthy person, C is set to 1. However, in order to simulate a patient, the fibre contractility in the LV was set to 0.4. The LV cavity volume and wall volume were set to 60 ml 150 ml respectively. The contractility of the RV was set to 0.8. These patient data were used to define the baseline in the simulation model. An overview is given in table 2.2. The amount of heart cycles that was simulated, was set to 50, since this was known from pas experience to be enough cycles for the system to reach a steady-state.

	R $[Pa \cdot s/m^3]$	L $[Pa \cdot s^2/m^3]$	C $[m^3/Pa]$
Heart Valves	$1 \cdot 10^6$		
Pulmonary Artery	$1.872 \cdot 10^6$	$1.25 \cdot 10^4$	$3 \cdot 10^{-8}$
Pulmonary Periphery	$1.81152 \cdot 10^7$		
Pulmonary Veins	$4 \cdot 10^4$	$9.375 \cdot 10^4$	$4 \cdot 10^{-7}$
Aorta, segment 1	$5.0 \cdot 10^6$	$5.625 \cdot 10^4$	$9.868 \cdot 10^{-9}$
Aorta, segment 2	$9.9 \cdot 10^6$	$5.625 \cdot 10^4$	$4.744 \cdot 10^{-9}$
Aorta, segment 3	$9.9 \cdot 10^6$	$5.625 \cdot 10^4$	$2 \cdot 10^{-9}$
Aorta, segment 4	$9.9 \cdot 10^6$	$5.625 \cdot 10^4$	$2 \cdot 10^{-9}$
Head Periphery	$6.3671 \cdot 10^8$		
Abdomen Periphery	$5.5771 \cdot 10^8$		
Kidney Periphery	$5.1742 \cdot 10^8$		
Leg Periphery	$6.3671 \cdot 10^8$		
Vena Cava Superior	$0.1 \cdot 10^6$	$1.736 \cdot 10^4$	$2.25 \cdot 10^{-7}$
Vena Cava Inferior, segment 1	$0.1 \cdot 10^6$	$1.736 \cdot 10^4$	$2.25 \cdot 10^{-7}$
Vena Cava Inferior, segment 2	$0.1 \cdot 10^6$	$1.736 \cdot 10^4$	$2.25 \cdot 10^{-7}$
Vena Cava Inferior, segment 3	$0.1 \cdot 10^6$	$1.736 \cdot 10^4$	$2.25 \cdot 10^{-7}$
Coronary Artery	$999 \cdot 10^6$	$1 \cdot 10^7$	$3 \cdot 10^{-11}$
Subendocardial Myocardium	$2400 \cdot 10^6$		$1.4 \cdot 10^{-8}$
Subepicardial Myocardium	$3500 \cdot 10^6$		
Coronary Vein	$700 \cdot 10^6$	$1 \cdot 10^7$	$7 \cdot 10^{-10}$

Table 2.1: Table of systemic values as determined by *Schampaert et al.*, with R the resistance, L the inertance and C the compliance.

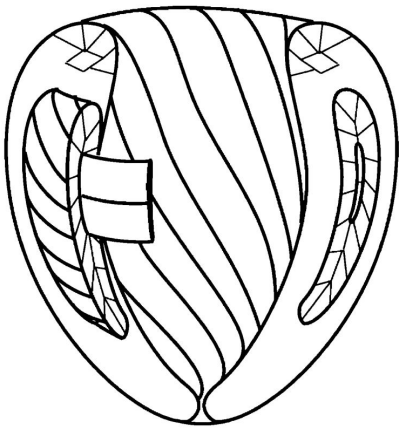

Figure 2.1: The representation of the fibre orientation of the LV, as described by *Arts et al. (2003)*.

	Left wall volume (ml)	LV contractility	RV contractility
Healthy	200	0.4	0.8
Pathological (Baseline)	150	1	1

Table 2.2: Parameter values for the heart simulations of both a healthy person and patient.

2.1.2 Baseline Validation

The baseline configuration that was created, had an output of 2.8 l/min and a mean arterial pressure (MAP) of 52 mmHg, which met literature criteria for CS patients [51]. Simulated differences were compared with a simulation of a healthy person with an output of 5.7 l/min and a MAP of 106 mmHg. The first comparison is shown in the PV-loops in figure 2.2. This figure shows a healthy situation of 138 mmHg systolic pressure, with a minimum and maximum volume of 71 ml and 142 ml respectively. Contraction and relaxation of the LV is isovolumetric. The PV-loop of the baseline has a maximum pressure of approximately 75 mmHg and minimum and maximum volumes of 118 ml and 153 ml respectively. The baseline also contains the expected isovolumetric contraction and relaxation in the PV-loop.

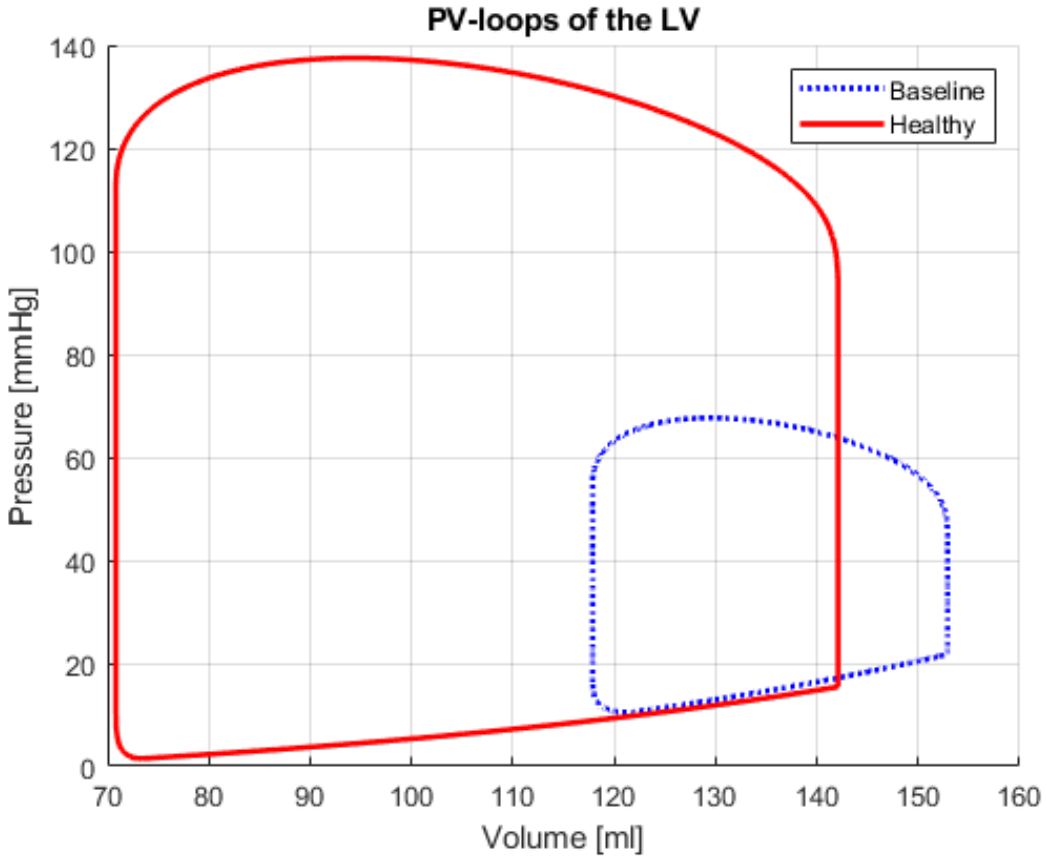

Figure 2.2: PV-loops of the left ventricle in both a healthy situation and patient situation.

Figure 2.3 shows the pressure values of the left ventricle, along with its preload and afterload for both the baseline and healthy situation. Aortic pressure decreases from 138 mmHg to 90 mmHg with the used settings. This figure also shows an increase in LA pressure, with decreasing aortic pressure.

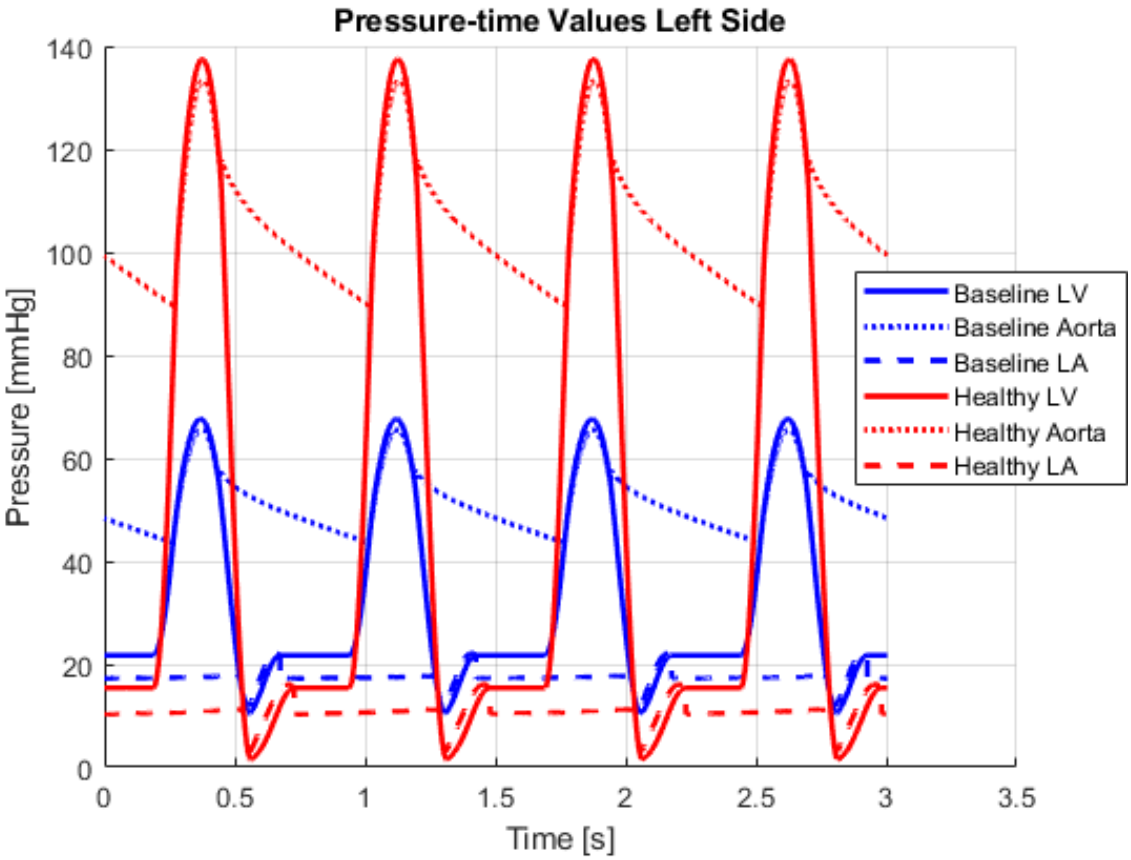

Figure 2.3: Pressure-time curves of the left ventricle, as well as the preload and afterload, for both the baseline and healthy situation.

Figure 2.4 shows the PV-loops of the right heart, for both the healthy simulation and the baseline. The healthy situation shows a maximum systolic pressure of 40 mmHg, with a minimum and maximum volume of 71 ml and 142 ml respectively. Contraction and relaxation of the LV is isovolumetric. The PV-loop of the baseline has a maximum pressure of approximately 33 mmHg and minimum and maximum volumes of 118 ml and 153 ml respectively. The baseline also contains the expected isovolumetric contraction and relaxation in the PV-loop.

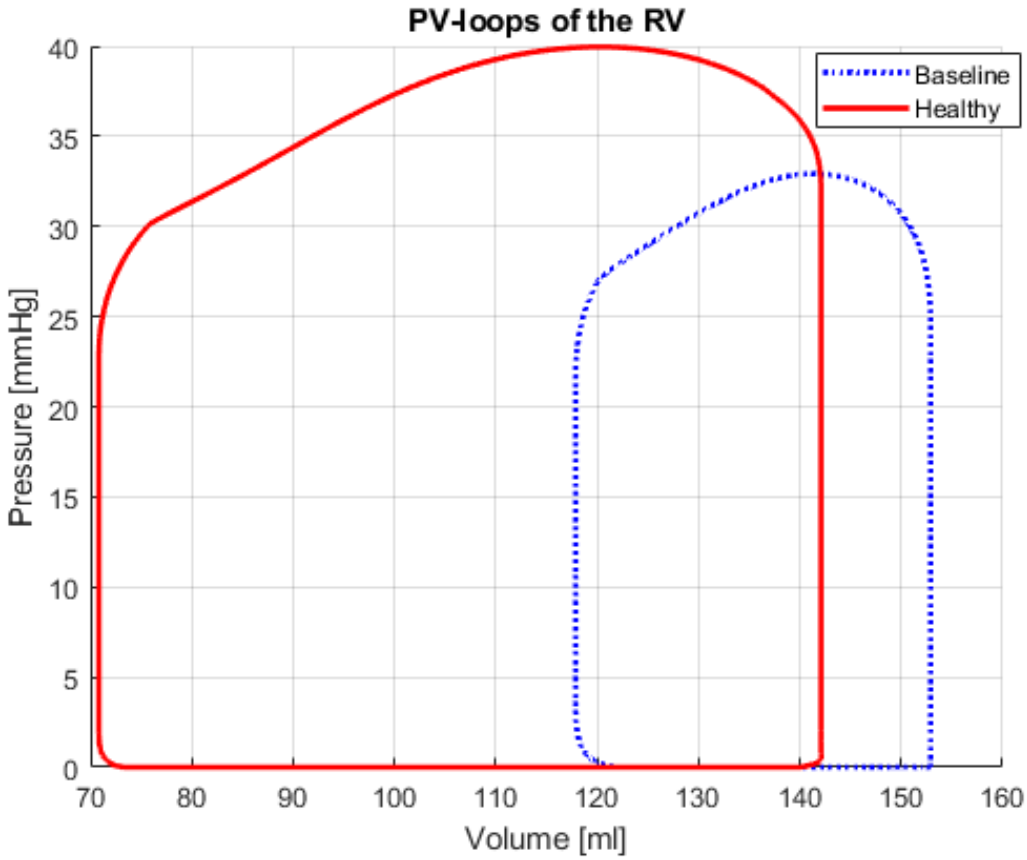

Figure 2.4: PV-loops of the left ventricle in both a healthy situation and patient situation.

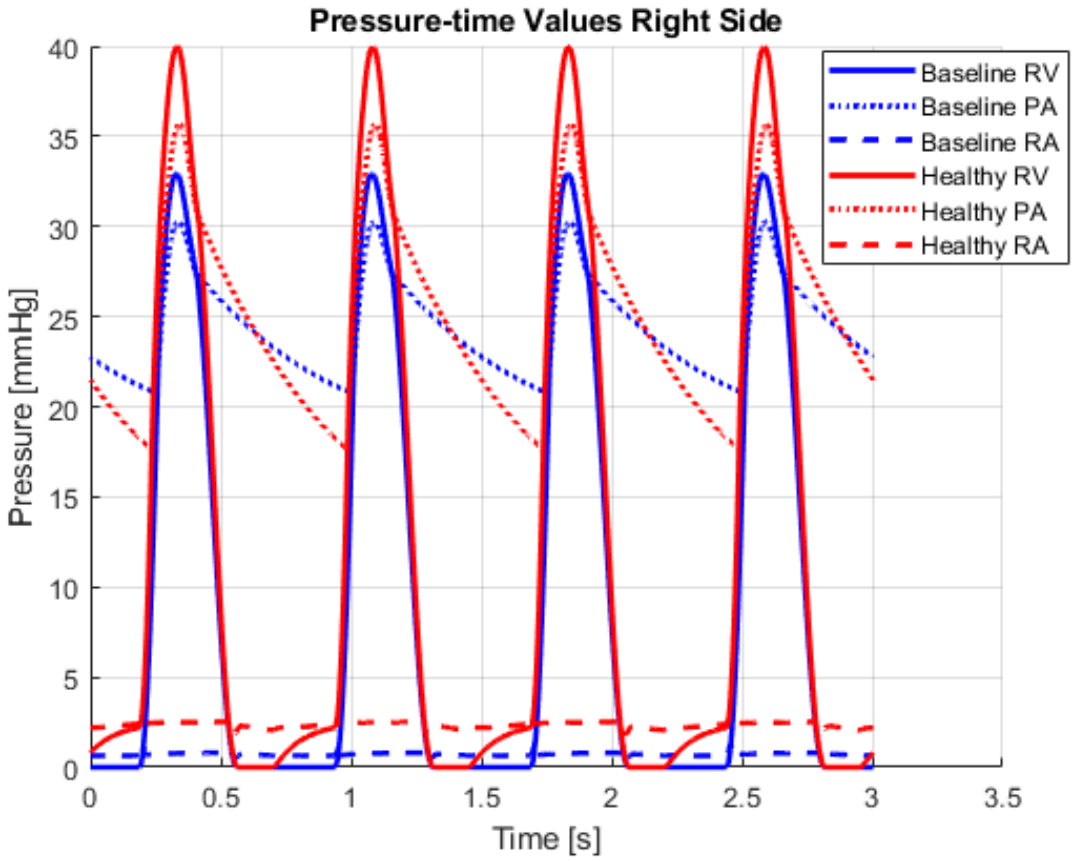

Figure 2.5: Pressure-time curves of the right ventricle, as well as the preload and afterload, for both the baseline and healthy situation.

Figure 2.5 shows the same pressure time plots for the right heart. This figure shows that the maximum systolic pressure decreases from 40 mmHg to 18 mmHg. RV preload is lower and afterload higher, compared to the baseline.

2.1.3 IABP Implementation

The IABP was implemented as done as *Schampaert et al. (2011)*. This was done by creating compliances at all four nodes of the aorta. These compliances were then connected to an additional nodal point P_{IABP}. During deflation, P_{IABP} was set at a value of -200 mmHg, while during inflation, it was set to 200 mmHg. The compliance of the IABP was dependent on its volume and extreme pressure values according to:

$$C_{IABP} = \frac{V_{IABP}}{P_{max} - P_{min}}$$

With V_{IABP} the volume, and P_{max} andP_{min} the respective maximum and minimum pressures of the IABP.

The volume of the IABP was set to 40 ml, with a length of 27 cm. The maximum and minimum pressures were set at 200 mmHg and -200 mmHg respectively. The inflation:deflation-

time ratio was set to 1:1, in order to provide maximum support[52]. The time it takes to both inflate and deflate was set to 0.135 s.

2.1.4 Impella 2.5 Implementation

The Impella 2.5 was implemented by defining outflow and inflow, from the LV and into the first node of the aorta.

The simulated flow was dependent on the pressure difference between the nodes of in and outflow. The flow-differential-pressure relation was described by *Pennings et al. (2013)* for selected devices that were based on both axial and centrifugal motors [53]. The flow dependence for the axial motors in ml/min, was described as:

$$q_{HAD} = \frac{a_1}{1 + \frac{1}{a_2} e^{\frac{\Delta P}{a_3 \cdot n^2}}} \cdot n \tag{2.1}$$

With ΔP the differential pressure in mmHg, n the rotation speed in RPM and a_1, a_2 and a_3 specific pump coefficients in l, [-] and $^{kg}/_{m}$ respectively. Estimation of coefficients, based on clinical data resulted in the values shown in table 2.3 [40], with maximum flow at 2.5 l/min.

Parameter	Value	Unit
a1	0.05	l
a2	10^2	-
a3	0.00212	$^{kg}/_{m}$
n	51000	RPM

Table 2.3: Parameter values for the implementation of the Impella 2.5.

These coefficients results in the flow-pressure curve as seen in figure 2.6.

For every time step, t_s, the effective volume displacement, $dV = q_{HAD} \cdot t_s$ was subtracted from the outflow-node (the LV) and added to the inflow node (the first aorta node).

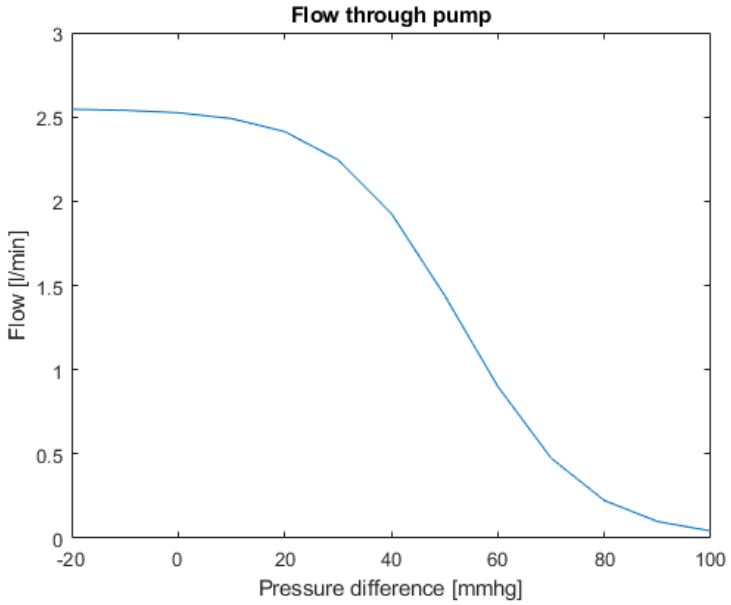

Figure 2.6: The flow-pressure relation for the Impella 2.5 at 51000 RPM.

2.1.5 PulseCath iVAC 3l Implementation

Since the iVAC 3l has a pulsatile flow profile, inflow and outflow were made time-dependent. For every heartbeat, inflow and outflow would have the same duration. Inflow would occur before and during the systole, while outflow would begin directly after end-systole. Storage of volume in the simulated reservoir of the device was allowed, with a limit of 40 ml. minimum volume was set to 0 ml.

It was assumed that for every heart beat, the iVAC 3l intake and ejection would be 40 ml. The flow of intake was described as:

$$q_{PC} = C \cdot sin(2\pi \cdot \frac{t_i}{t_{cycle}}) \qquad 0 \leq \frac{t_i}{t_{cycle}} < 0.5 \tag{2.2}$$

With C the scale factor to have 40 ml per heart beat as total flow, t_i the time step at moment i and t_{cycle} the duration of one heartbeat. During the time period $0.5 \leq \frac{t_i}{t_{cycle}} < 1$, ejection was described as in equation 2.2. Inflow would then be 0.

2.1.6 TandemHeart Implementation

The TandemHeart is simulated in a similar way as the Impella 2.5. Flow was described as continuous, but pressure dependent. Like the flow for the Impella 2.5, the flow was made pressure dependent, based on the work of *Schampaert et al.* though with pressure dependence based on centrifugal pumps. This relation was described as:

$$q_{HAD} = \frac{-b_2 - \sqrt{(b_2)^2 - 4b_1\left(b_3 - \frac{\Delta P_{LVAD}}{n^2}\right)}}{2b_1} \cdot n \tag{2.3}$$

With ΔP the differential pressure in mmHg, n the rotation speed in RPM and b_1,b_2 and b_3 specific pump coefficients in ${}^{kg}/_{m \cdot L^2}$, ${}^{kg}/_{m \cdot L}$ and ${}^{kg}/_{m}$ respectively. Estimation of coefficients,

based on clinical data resulted in the values shown in table 2.4, with a flow of 4 l/min at 0 mmHg pressure gradient [40].

Parameter	Value	Unit
b1	-3.22	$^{kg}/_{m \cdot l^2}$
b2	$10.6 \cdot 10^{-2}$	$^{kg}/_{m \cdot l}$
b3	1.05	$^{kg}/_{m}$
n	7500	RPM

Table 2.4: Parameter values for the implementation of the TandemHeart.

These coefficients result in the flow-pressure curve as seen in figure 2.7.

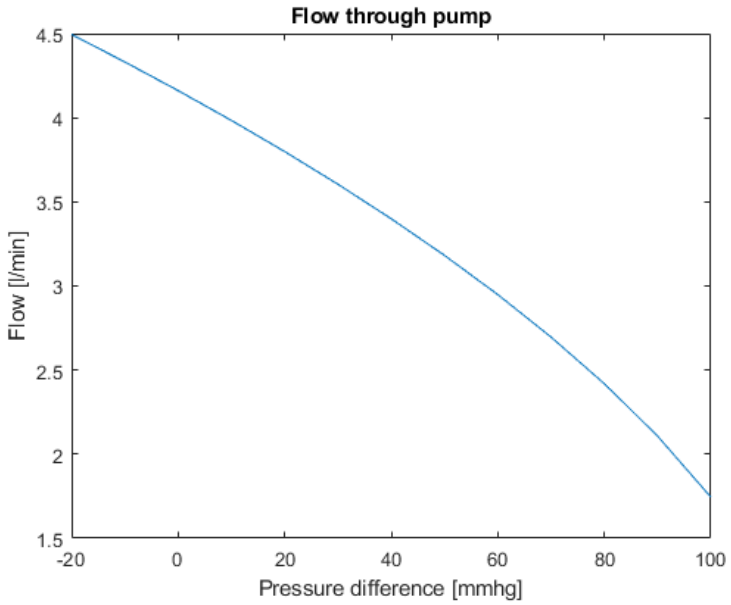

Figure 2.7: The flow-pressure relation for the TandemHeart.

2.1.7 Integrating Devices

With the exception of the IABP, these devices draw volume from the nodal point at the inlet and adds this volume to the nodal point outlet. In order to stabilise this sudden volume change, two additional nodal points are created. These nodes link the device with its corresponding inlet and outlet, along with a resistance. This set-up is shown in figure 2.8. The resistances were given a value of $1 \cdot 10^6 \frac{Pa \cdot s}{m^{-3}}$, which was the same as those of the heart valves.

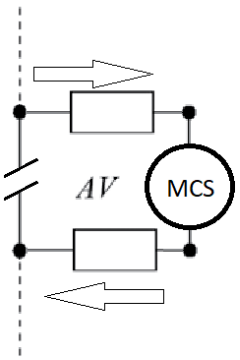

Figure 2.8: The integration of an MCS device, along with the additional nodal points.

2.1.8 Acquiring Data

Of the 50 heart cycles that were simulated, the last four were used for evaluation and validation. Data were saved and stored into .mat files, so that all data could be loaded later. Data that were used, were PV flow, AV flow, arterial pressure, vena cava pressure, LV volumes and pressures and flow through each device. From these data, mean flow, MAP, PV-loops and PP were calculated. Energy values were also calculated as:

LV work done	$W_{LV} = \int_{V_{sys}}^{V_{dia}} P_{LV} dV$
Systemic energy uptake	$E_{system} = d\hat{P} \cdot \hat{q} \cdot t$
MCS device work done	$E_{device} = E_{system} - W_{LV}$

With $d\hat{P}$ the mean pressure difference between the aorta and the vena cava and $\hat{q}$ the mean flow.

2.2 Mock-loop model

2.2.1 System Properties

For the mock-loop experiment, the experimental set-up of the TU/e was used. This experimental set-up uses cylindrical, silicone rubber tubes, which represent the arteries and veins. The arterial tube had a length of 45 cm, a diameter of 23 mm and a wall thickness of 1 mm in order to have physiological material properties, similar to those of the arterial wall. System compliances were created with closed reservoirs, partially filled with air. System resistances were created with tapered screws, which partially blocked the in- and outlet of each reservoir. All compliances and resistances could be adjusted manually, in order to create physiological values. Heart beats were simulated by two piston pumps, controlled by servo motors, representing the right- and left ventricles. Motion of these motors could be controlled per time step, resulting in accurate control of piston locations. The right and left atria are modelled with compliance chambers, making the atria passive components. All heart valves were modelled with silicon rubber valves, preventing back-flow. Further details of this experimental set-up can be found in the original article by *Schampaert et al. (2011)* [49].

This set-up was controlled with Matlab 2006a, using Simulink. Routines and settings were written in C code. The PC's operating system is CentOS 6, which allows real time input and output processing of the servo motors and sensors. These sensors measured pressure and flow in the aorta, venous system, RA pulmonary system and LA. Pressure was also measured in both ventricles, as well as both piston displacements, the latter enabling volume calculation. All sensors were connected to the PC, through signal amplifiers. The performed measurements had a sampling rate of 1000/s

The used MCS devices for this experiment, were the Impella 2.5, the 50cc IABP, the PulseCath iVAC 3l and the TandemHeart. These devices were controlled, using appropriate drivers. A baseline experiment, meaning an experiment without a HAD implemented, was also performed for reference and comparison.

2.2.2 Preparations and Settings

Connecting Devices

The Impella 2.5 and PulseCath were connected to a separate outlet of the cylinder which represents the LV and a branch of the arterial tube, distal from the AV. The TandemHeart was connected to the outlet of the LA (inlet) and the most proximal part of the aorta (outlet). The IABP was placed into the aorta, through a distal inlet.

Mock-Loop Preparation

Before measurements, all compliance tanks were filled, after which all pressure signals were set to zero. A pressure of 7 mmHg was then set by adding air into the compliance tanks. The amount of air in the compliance tank would then give a physiological compliance in that part of the system. A CS patient was then simulated, in order to set the resistances of the system. These resistances were adjusted, until an arterial pressure of 80/35 mmHg was reached, as well as a mean flow of approximately 3 l/min.

Device Preparations

All devices were not switched on, until the simulation had reached a steady-state. In this case, a 'steady-state' is defined as a state at which all future heart cycles have an identical pressure and flow profile. The moment of steady-state was manually determined.

All devices were tested at full capacity. Therefore, The IABP was set at an assist rate of 1:1, in accordance with the simulation model. The Impella 2.5 and the TandemHeart ran at their maximum speed of 51000 RPM and 7500 RPM respectively.

Mock-Loop Settings

After preparations were done as described above, specific data, a CS patient could be simulated. This was done, by lowering the contractility of the fibres in the one-fibre model from $c = 1$ to $c = 0.7$ for the LV and from $c = 1$ to $c = 0.8$ for the RV. The LV cavity volume and wall volume were set to 60 ml and 125 ml respectively, as was done in the simulation model. The contractility of the RV was also set to 0.8. This setting was defined as the baseline.

Acquiring Data

After the system was initialised, a steady-state was reached and a connected MCS device was switched on. Past experiences showed that a steady-state is ready in less than 50 s. Measurements therefore occurred for $100s$, including margin. This was considered more than enough time to reach a steady-state for the system again with an active MCS device. Results of this experiment, used the data of the last four complete heart cycles. Data that were measured, were mean flow, mean arterial pressure (MAP), Pulse pressure (PP), coronary flow and LV volumes and pressures.

2.3 Experiment Protocol

After the system was calibrated, the heart properties were set to an LV contractility of 0.7, the LV cavity volume and wall volume set to 60 ml and 125 ml respectively and the RV contractility set to 0.8, simulations commenced. After the system had reached a steady-state, MCS was switched on. After a steady-state was reached again, measurements were performed. Data that was used, was flow through all valves, arterial pressure, coronary flow and LV volumes and pressures.

Chapter 3

Results

3.1 Simulation Model

3.1.1 Steady-State Confirmation

In order to determine whether the simulation model has reached a steady-state, the maximum flow through the PV, per heart cycle, was plotted for all simulations. This can be seen in figure 3.1. The maximum flow through the AV is also plotted and can be seen in figure 3.2.

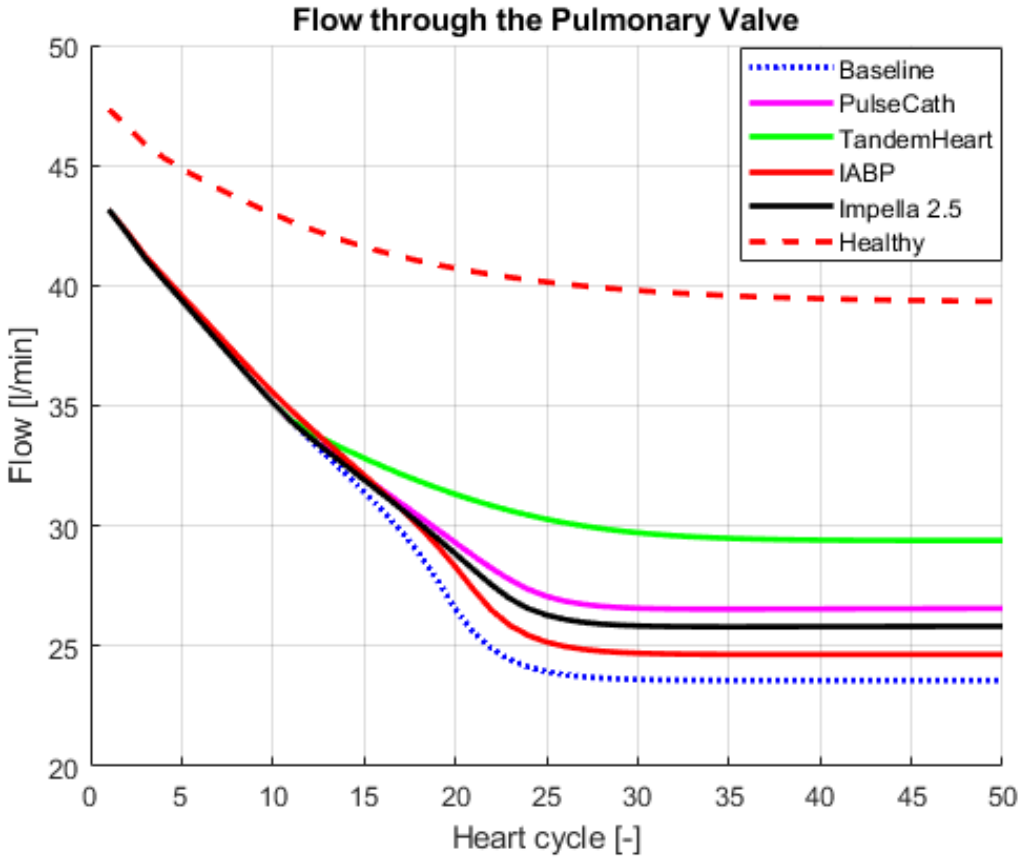

Figure 3.1: Maximum flow through the pulmonary valve for every heart cycle.

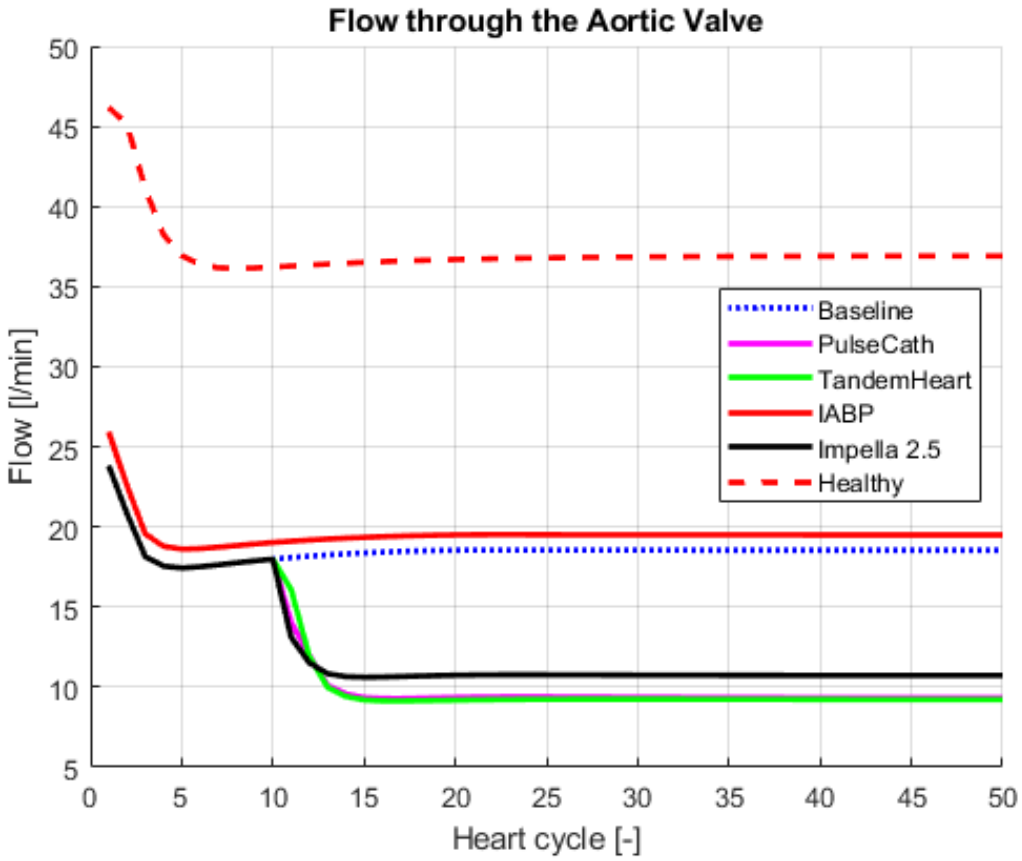

Figure 3.2: Maximum flow through the aortic valve for every heart cycle.

For all simulations, figure 3.1 shows a consistent flow through the PV for every heartbeat, during the last heart cycles. Figure 3.2 shows a consistent flow though the AV as well. It was therefore assumed that the system was in steady-state during the last four heart cycles, for all simulations. All data that are discussed below, were taken from the simulation of these last four cycles.

3.1.2 Mean Flow and Mean Arterial Pressure

For the last heart cycles, the mean flow through the PV and the MAP were determined. In order to see consistency over these last cycles, while still being able to see detail, four cycles have been plotted. The results are shown in the bar plot of figure 3.3.

This bar plot shows that the baseline has a mean flow of approximately 2.7 l/min and a MAP of 50 mmHg, which was considered pathological. Furthermore, the flow and MAP values for the MCS simulations show higher values, especially the TandemHeart simulation, with a mean flow of 3.9 l/min and a MAP of 66 mmHg. Both the Impella and PulseCath show no significant differences in mean flow and MAP. The IABP has the lowest influence on mean flow and MAP. However, just like the other devices, both values of the IABP are higher compared to the baseline.

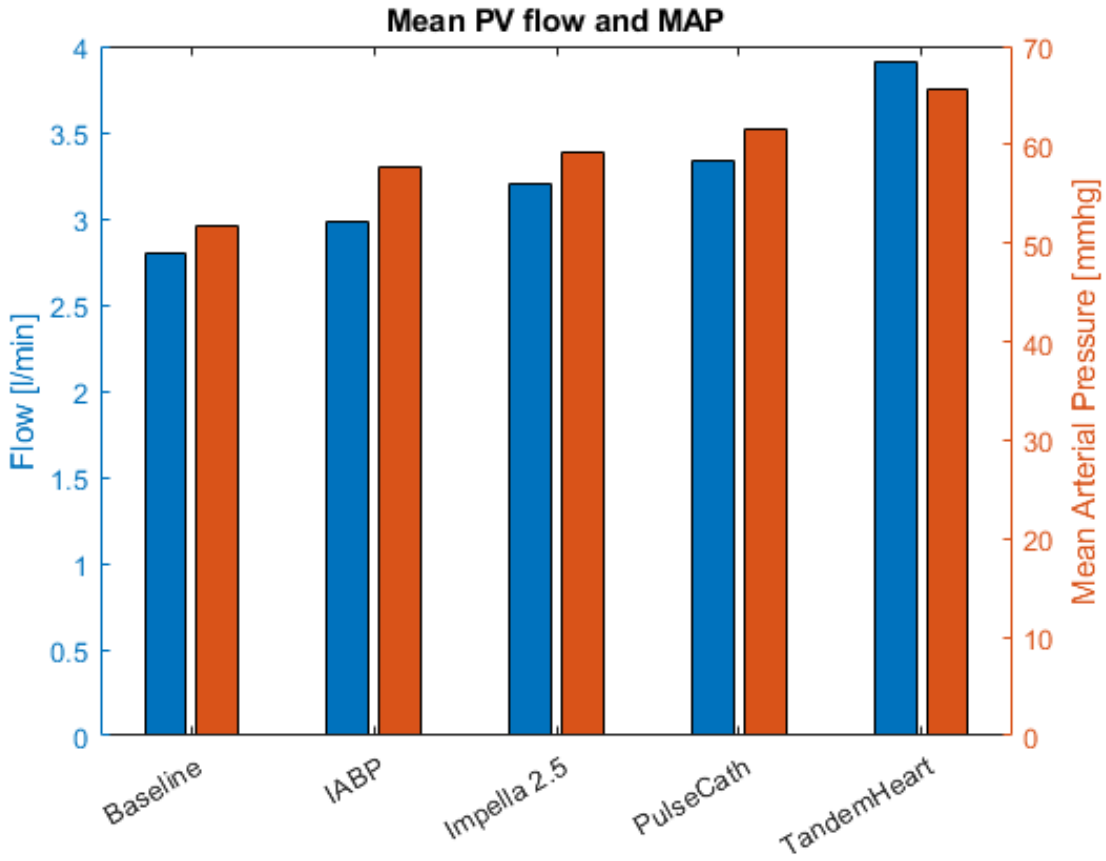

Figure 3.3: Bar plot of the mean flow through the pulmonary valve and the mean arterial pressure.

3.1.3 Pressure-Volume Loops of the Left Ventricle

The pressure-volume loops (PV-loops) for the last heart cycle, have been compiled for all simulations. These PV-loops are shown in figure 3.4

The PV-loops that are shown, have their extreme values in a similar range, though the loops of the MCS devices, might be different in form. The maximum volume of the LV with IABP implementation does not seem to change, though the minimum volume is lowered to a value of 115 ml, resulting in a higher SV. Pressure-wise, the PV-loop of the IABP does not differ from the baseline.

The PV-loop under Impella support shows multiple differences, compared to the baseline. First of all, there are no isovolumetric states, since the Impella continuously decreases LV volume. There is also a high decrease in maximum volume to 142 ml. The minimum volume is slightly lowered to 115 ml. There is no difference in extreme pressure values, compared to the baseline

The PulseCath also lowers the minimum and maximum LV volume. These are 110 ml and 146 ml respectively. Furthermore, the right side of the PV-loop shows no isovolumetric contraction, due to suction of the PulseCath. Suction occurs during relaxation as well, until a pressure of 45 mmHg. After that, the relaxation is isovolumetric again. All pressure values,

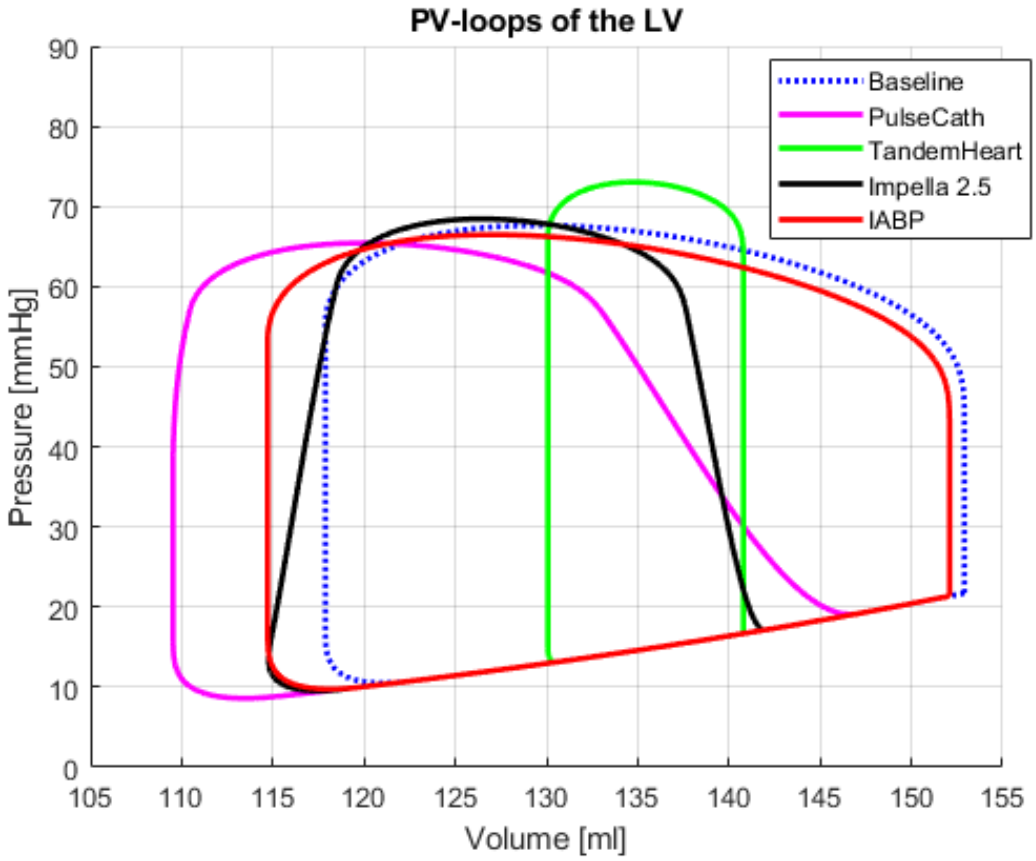

Figure 3.4: Pressure Volume loops during the last cycles for all simulations.

including extreme values are comparable to those of the baseline.

The PV-loop that is most different from the that of the baseline, is the one of the TandemHeart, with a maximum volume of 141 ml and a minimum volume of 130 ml. These volumes give a LV stroke work of 11 ml. The maximum systolic pressure is 73 mmHg, which is higher compared to the baseline. This PV-loop shows isovolumetric states.

3.1.4 Aortic Pressure and Pulse Pressure

In order to evaluate the aortic pressure and PP, the aortic pressure is plotted in figure 3.5.

The aortic pressure of the baseline reaches a maximum of 65 mmHg during systole. After reaching this maximum, pressure gradually drops during the rest of the systole, followed by the relaxation, to a minimum pressure of 45 mmHg. Pressure rapidly rises again after the beginning of the diastole until the maximum pressure is reached again.

For the IABP, the pressure rises from 64 mmHg during inflation of the balloon, which occurs during the diastole. After a pressure decrease to 54 mmHg, the pressure rapidly rises again, to a value of 63 mmHg. Pressure starts to drop gradually to 61 mmHg, the moment the balloon started to deflate. Rapid pressure drop to 43 mmHg occurs. After this, pressure rises rapidly due to the start of the new systolic phase. The minimum pressure of the IABP simulation is similar to the minimum pressure of the baseline.

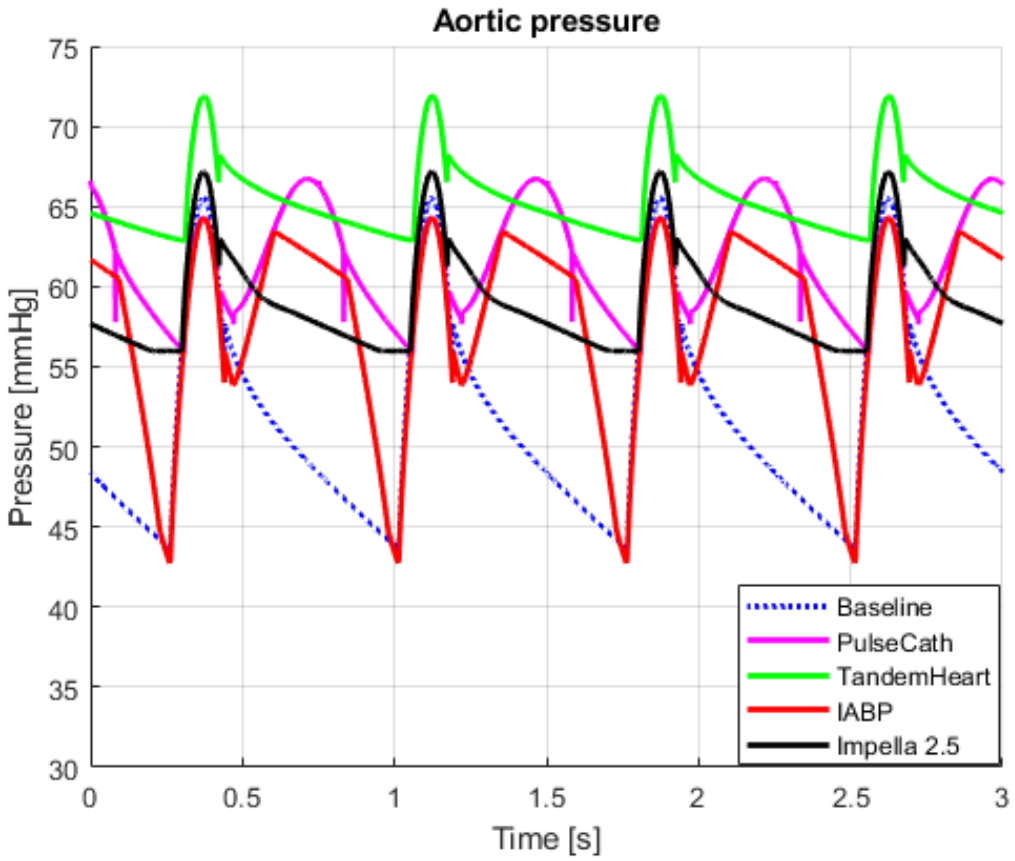

Figure 3.5: Pressure-time plot in the most proximal nodal point of the aorta for all simulations.

The PulseCath rapidly increases the aortic pressure from 53 mmHg to 67 mmHg during the diastole, when outflow into the aorta occurs. The pressure curve shows a sine wave. Pressure then decreases to 61 mmHg until outflow stops. The pressure then drops to 56 mmHg. Pressure rises again during the next cycle. However, this occurs later compared to the simulations of the baseline and IABP.

For every time step, the Impella simulation has a higher aortic pressure during a cycle compared to the baseline. This is especially the case during the diastole, where the pressure decreases less rapidly for the Impella simulation. The end diastolic pressure is 56 mmHg.

The TandemHeart shows similar results to those of the Impella, however, with a significant difference in pressure. After the simulation reaches a maximum systolic pressure of 72 mmHg, pressure drops rapidly, similar to the Impella results. Pressure still drops during the diastole, but more gradually compared to the baseline.

PPs of all simulations are shown in the bar chart of figure 3.6. This shows that the IABP approximately has the same PP as the baseline, with a value of 21 mmHg. Other devices show a significantly lower PP value of 9 to 11 mmHg.

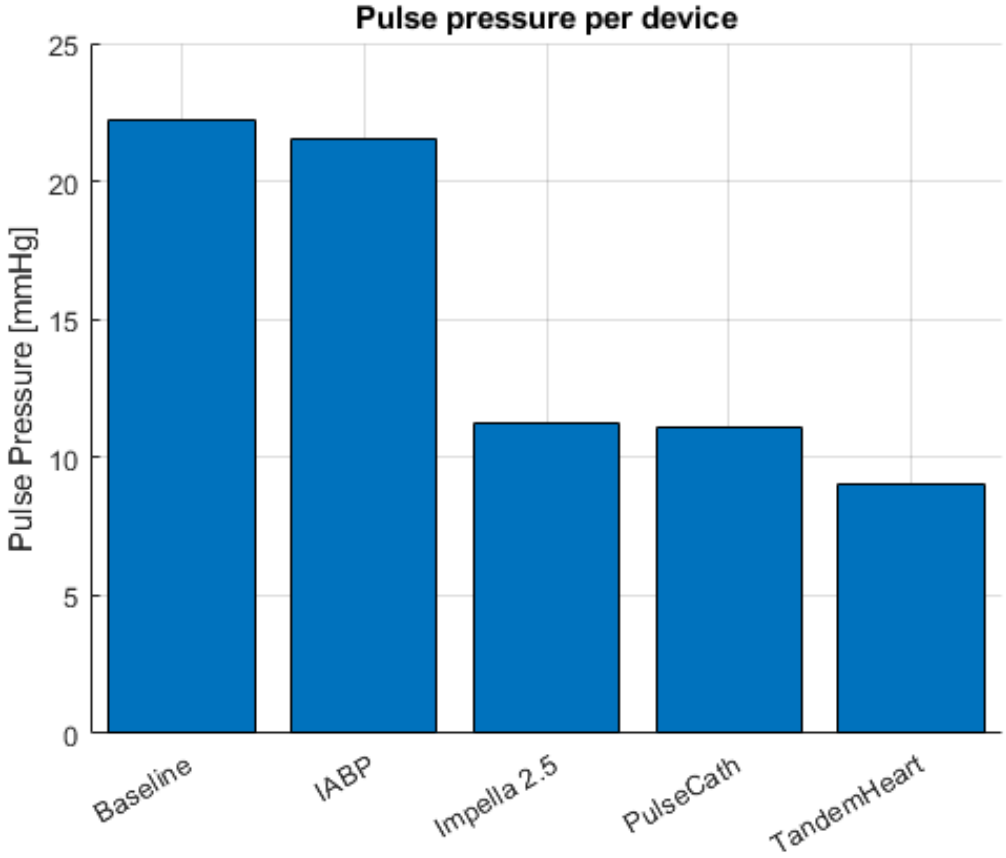

Figure 3.6: Pulse pressure values for all simulations.

3.1.5 Device Output

With the exception of the IABP, the evaluated devices all pumps with a certain flow rate. The flow through these devices is discussed in figure 3.7.

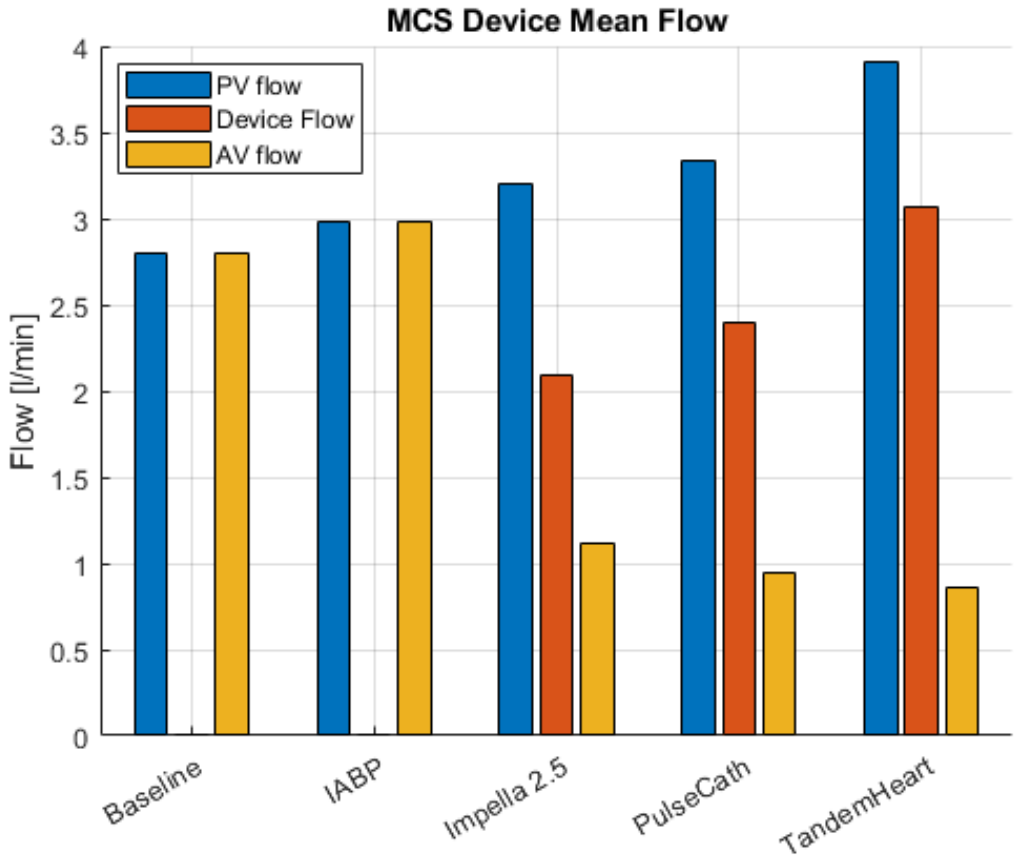

Figure 3.7: Mean flow through the pulmonary valve, the MCS device and the Aortic valve. Note that MCS flow is not applicable for the baseline and IABP.

This figure shows the flow in the PV, as was shown in figure 3.3, along with the flows through the MCS device and the aortic valve. This figure shows a higher device flow along with a higher PV flow, but lower AV flow. The combined device flow and AV flow equals the PV flow.

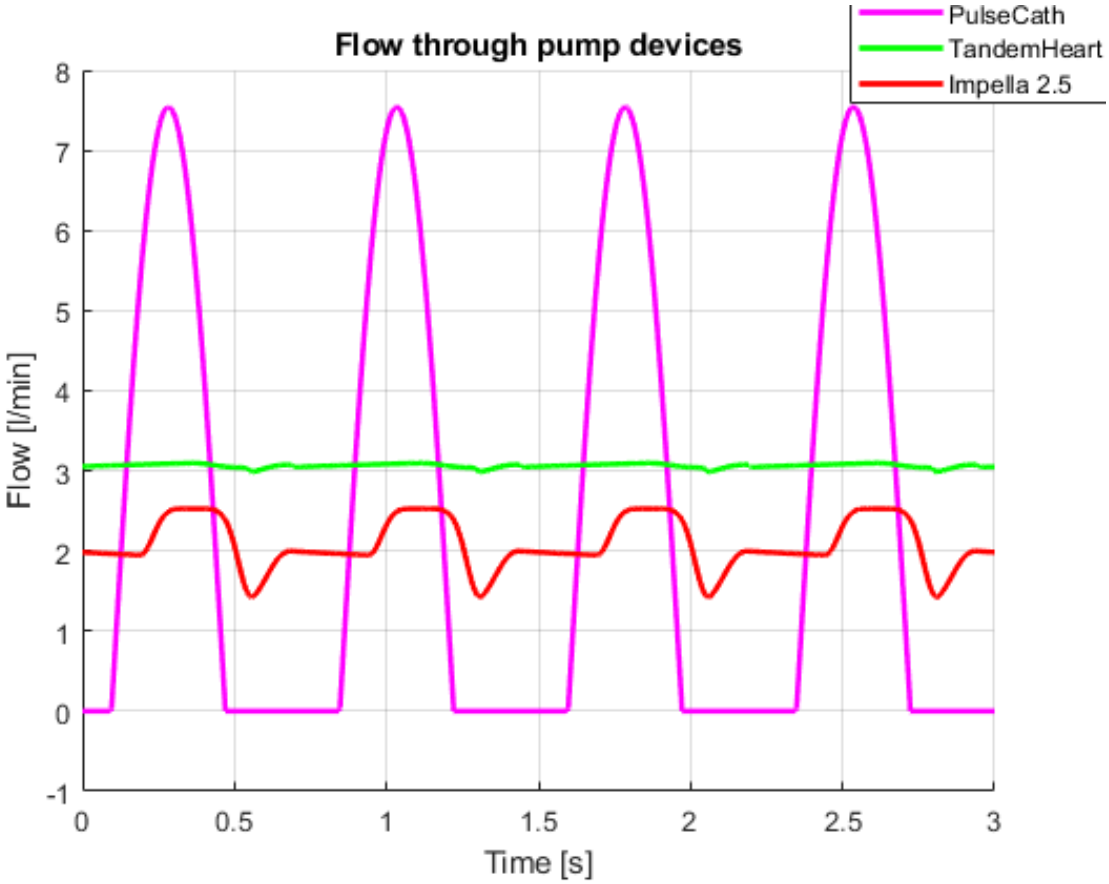

Figure 3.8: Flow-time plot into the MCS device. Note that MCS flow is not applicable for the baseline and IABP.

The flow-time plots for these MCS devices were also evaluated. The flows into these devices are shown in figure 3.8. This figure shows an almost constant flow of 3 l/min through the TandemHeart, whereas the PulseCath and Impella have time-dependent flows. The PulseCath flow shows a half-sine function. The Impella flow shows a time-dependency of a more complex nature.

3.1.6 Left Ventricle Work

The mechanical work done by the LV and MCS devices was also evaluated. The amount of work done, by the LV and the MCS device, for each cycle is shown in figure 3.9. The amount of energy that was added to the system is shown as well.

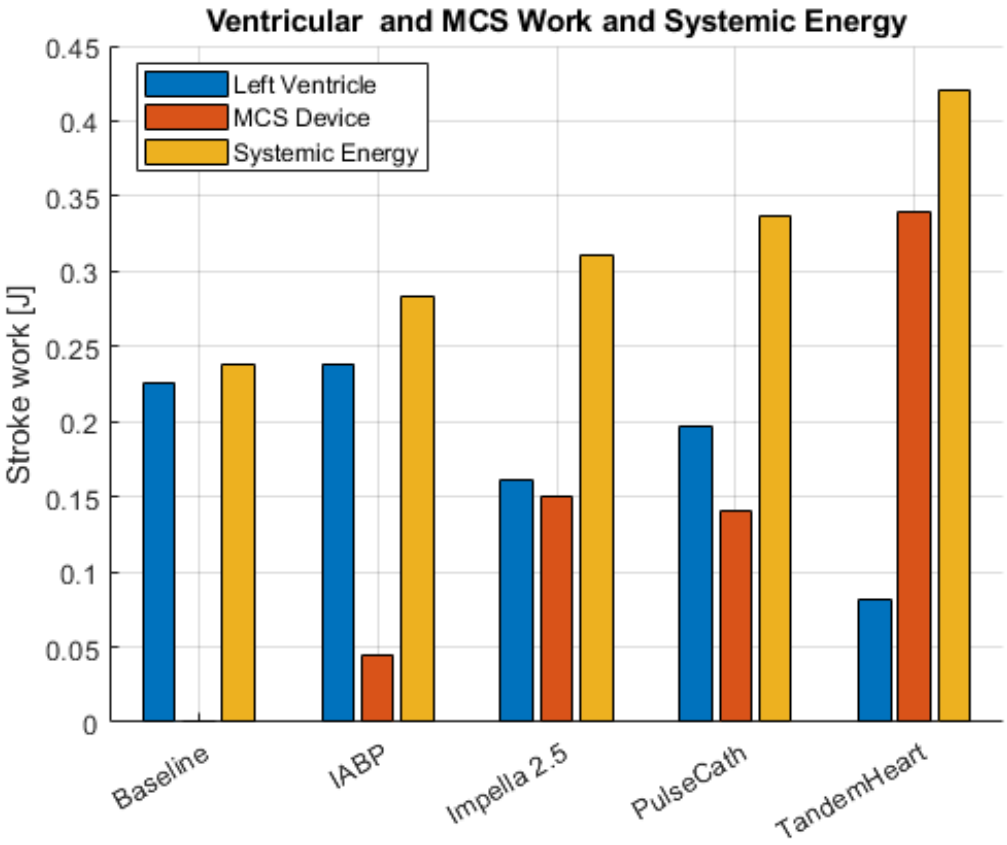

Figure 3.9: Flow-time plot into the MCS device. Note that MCS flow is not applicable for the baseline and IABP.

The baseline shows an that the LV work done and systemic energy uptake differ. The difference between these values is 0.01 J, giving a relative difference of 5%. With the exception of the IABP, simulations with MCS devices implemented, show lower LV work done and higher systemic energy uptake. The ratios between LV work done and systemic uptake are shown in table 3.1.

	Ratio of work done by LV
Baseline	0.95
IABP	0.84
Impella 2.5	0.52
PulseCath	0.58
TandemHeart	0.19

Table 3.1: Relative work done by the left ventricle.

3.2 Mock-Loop Model

3.2.1 Confirmation of Similarity

In order to evaluate the similarity of all simulations, at the time when MCS was switched off, the PV loops of the LV were plotted. These are shown in figure 3.10.

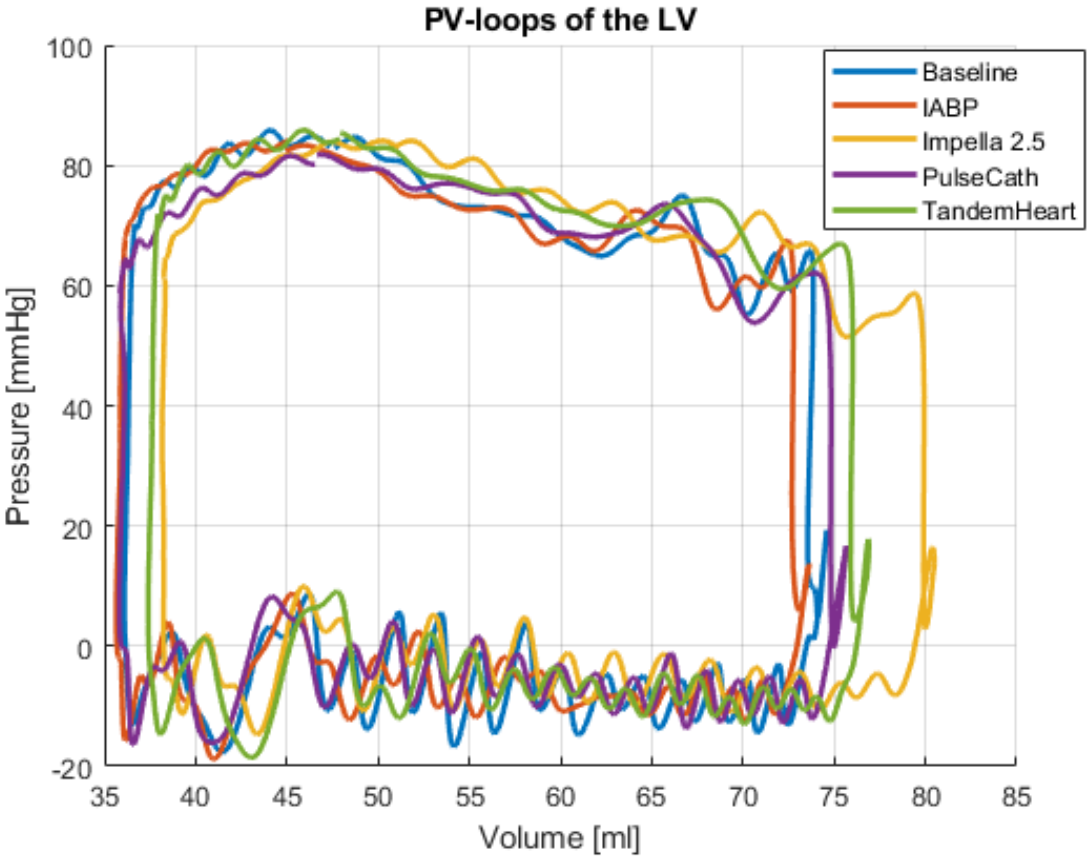

Figure 3.10: PV-loops for all simulations without MCS.

This figure shows that all PV-loops are between pressure values of 85 mmHg and -20 mmHg. Volume values are between the range of 35 ml and 82 ml. These PV-loops show the same shape. During the diastole, the pressure values oscillate. Oscillation occurs during the diastole as well, but this is less present. All PV-loops show isovolumetric contraction and relaxation.

The pressure-time curves of the aorta were also evaluated. This is shown in figure 3.11.

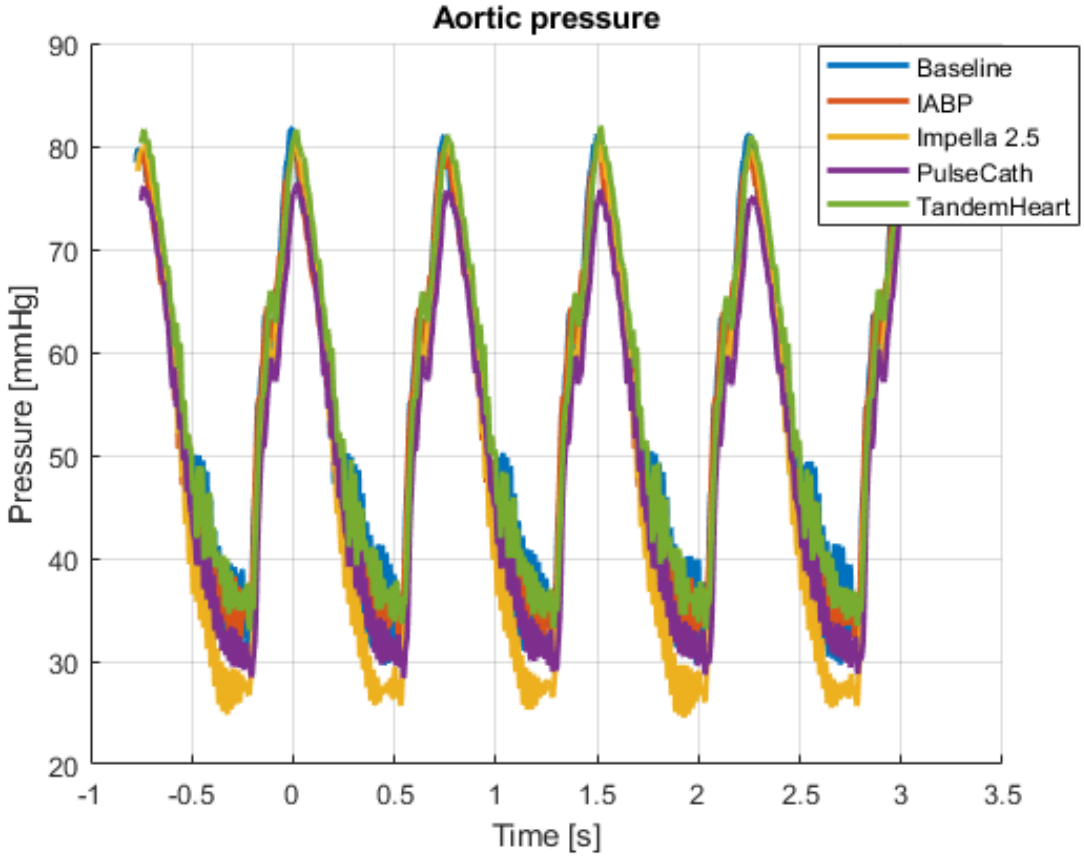

Figure 3.11: Pressure-time curves of the aorta for all simulations without MCS.

This figure shows that the peak systolic pressure differ with a maximum of 6 mmHg. The end diastolic pressure differs with 8 mmHg. All curves show similar behaviour.

Since all simulations showed PV-loops and arterial pressures of close resemblance, comparison of MCS results with the shown baseline was therefore considered valid.

3.3 Mean Flow and Mean Arterial Pressure

For the last four heart cycles, the mean flow through the PV and the MAP were determined. The results are shown in the bar plot of figure 3.12.

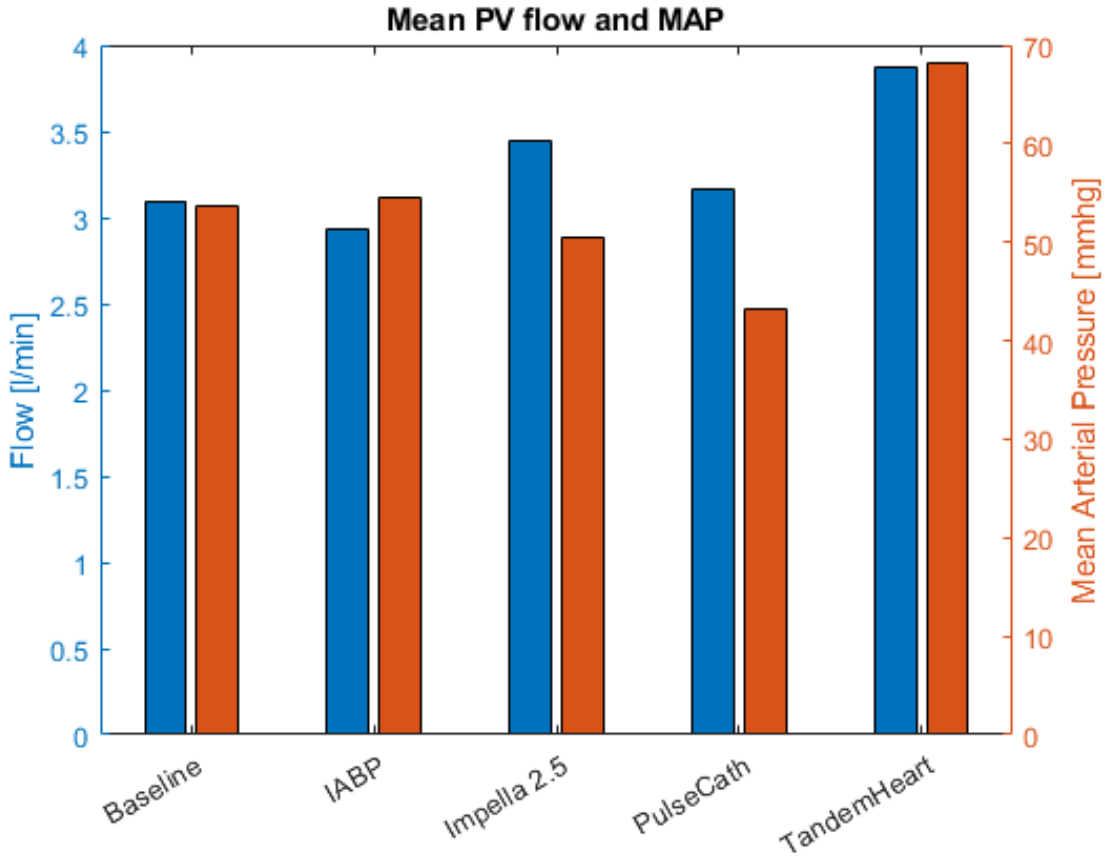

Figure 3.12: Bar plot of the mean flow through the pulmonary valve and the mean arterial pressure.

The baseline has a mean flow of approximately 3.1 l/min with a MAP of 54 mmHg. This is considered pathological. The figure also shows higher flow values for the Impella 2.5 and TandemHeart simulations. The PulseCath does not seem to have effect on the mean flow and the IABP seems to lower the mean flow. The TandemHeart effectively highers the mean flow to 68 mmHg. The IABP does not seem to have effect on the MAP and the Impella and PulseCath lower the MAP.

3.3.1 Pressure-Volume Loops of the Left Ventricle

For the last heart cycle of each simulation, the PV-loops of the LV have been plotted. These PV-loops are shown in figure 3.13.

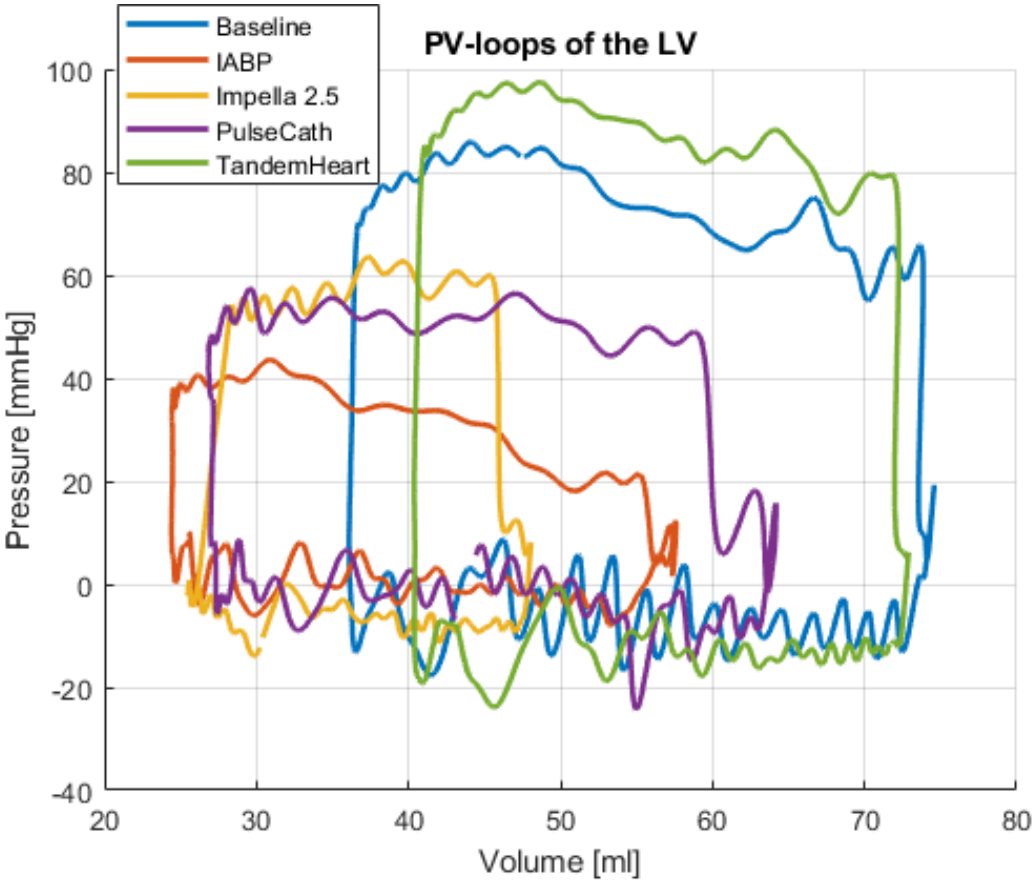

Figure 3.13: PV-loop of all simulations with MCS.

In comparison to the baseline, the TandemHeart has a higher maximum systolic pressure, which is 96 mmHg. The maximum volume does not seem to change, however, the minimum volume of the LV with TandemHeart support rises. This leads to a lower SV of the LV. For all other MCS simulations, both the maximum systolic pressure and the maximum volume drops. The Impella supported PV-loop does not show isovolumetric contraction and relaxation. The PulseCath supported PV-loop does not show isovolumetric contraction, but does show isovolumetric relaxation. The IABP supported PV-loop has the smallest extreme volume values and has the lowest maximum systolic pressure.

3.3.2 Aortic Pressure and Pulse Pressure

The pressure-time plots for every simulation were plotted and are shown in figure 3.14.

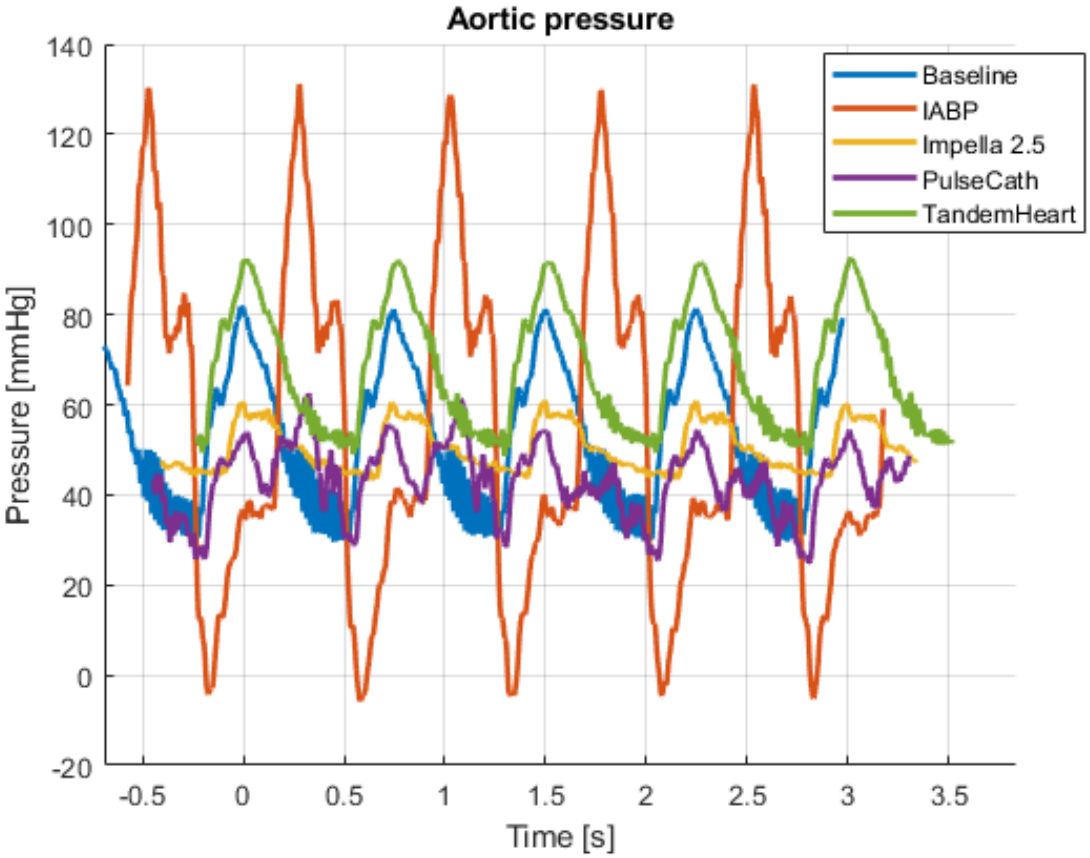

Figure 3.14: Pressure-time plots of the aorta for all simulations.

These pressures change over time, differently for each simulation. The baseline has a peak systole of 80 mmHg and a minimum diastolic pressure of 35 mmHg.

When this is compared to the simulation with PulseCath support, a more continuous signal is shown. During the systole, this reaches a pressure of 55 mmHg, before this pressure drops to 30 mmHg. During the diastole, the pressure rises again, until a value of 51 mmHg is reached. After this, pressure drops again until the beginning of the new cycle.

The Impella shows a more continuous pressure as well, with pressure varying from 60 mmHg to 45 mmHg. The shape of this graph is otherwise similar to that of the baseline.

The TandemHeart shows the same shape of this graph as well, only with higher pressure values. Pressures vary from 92 mmHg to 50 mmHg.

Lastly, the IABP shows a different relation, with pressures varying from 130 mmHg to -4 mmHg. During systole, the aortic pressure rises from -4 mmHg to 40 mmHg. During inflation of the balloon, pressure rapidly rises to 130 mmHg. After deflation, the aortic pressure drops to -4 mmHg again, with a sudden rise around 80 mmHg.

The PP is also plotted for each simulation. This is shown in figure 3.15.

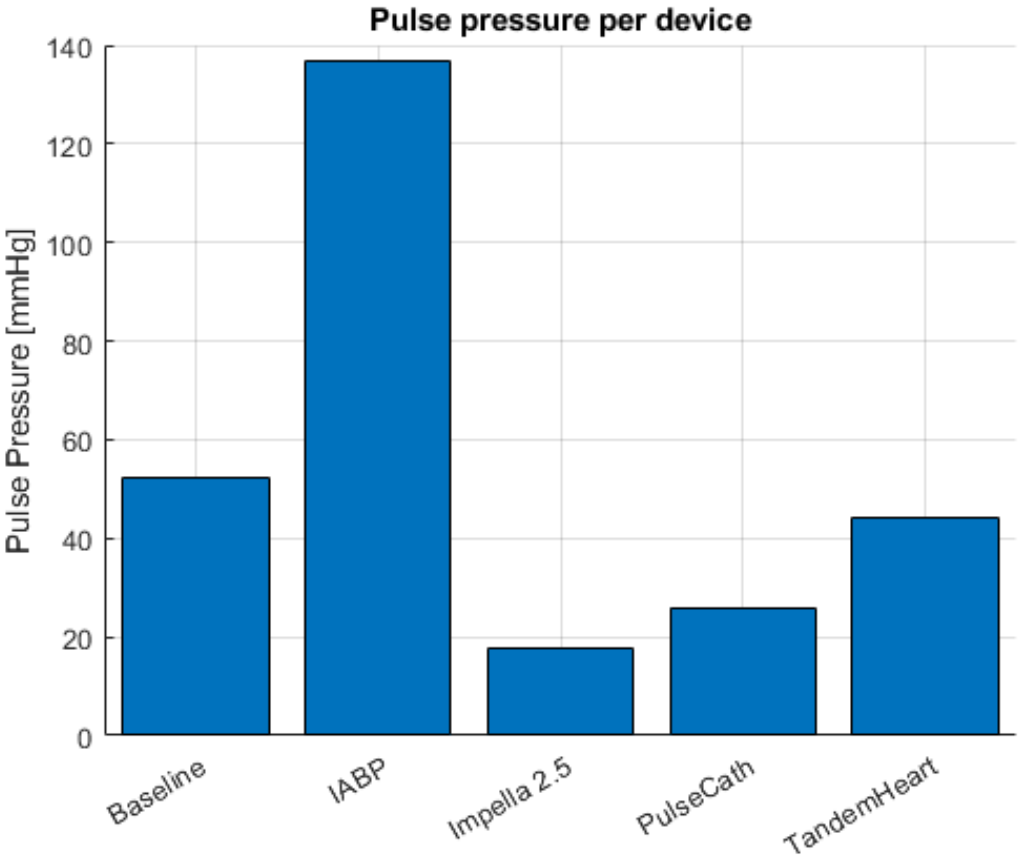

Figure 3.15: Pulse pressure values for all simulations.

The baseline has a PP of 52 mmHg. With the exception of the IABP, MCS seems to lower the PP, especially the Impella, with a PP of 18 mmHg. The IABP has a PP of 137 mmHg, about 2.5 times as high as the baseline.

3.3.3 TandemHeart Flow

The flow through the TandemHeart was measured. The results of this are shown in figure 3.16.

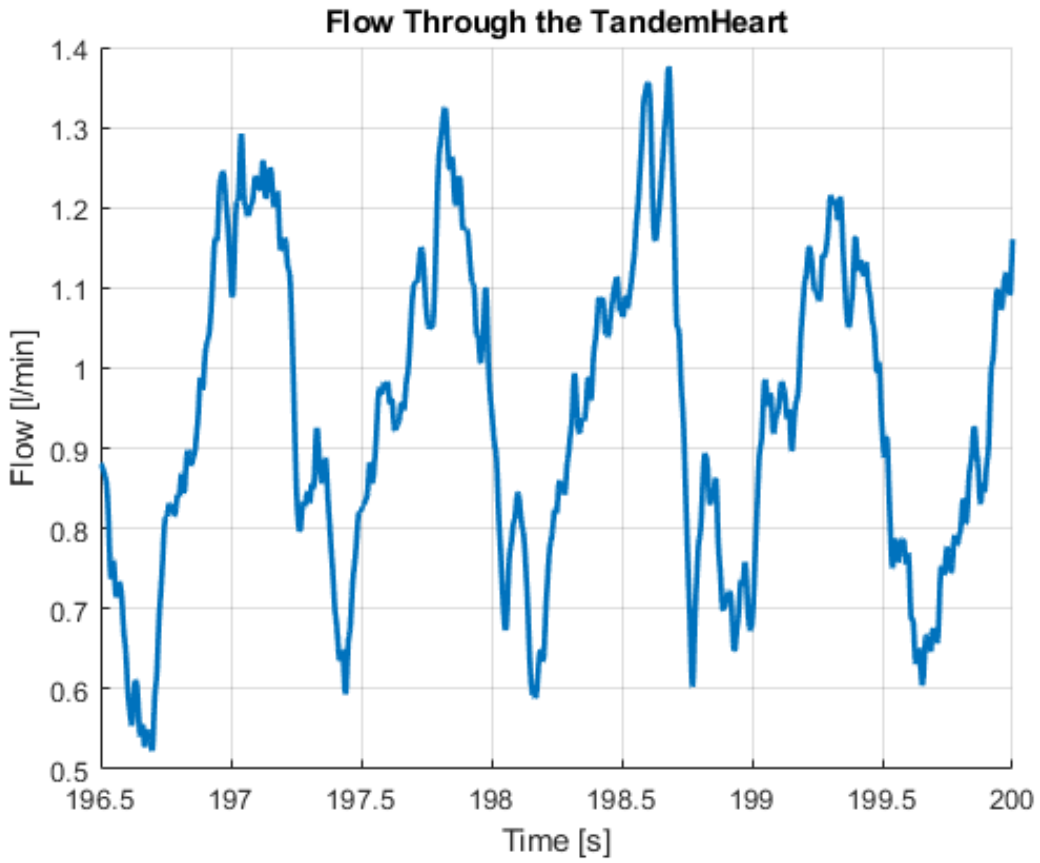

Figure 3.16: Flow Through the TandemHeart during MCS.

The flow through the TandemHeart varies between 0.6 l/min and 1.3 l/min. The mean flow through the TandemHeart was 1 l/min. The flow profile changes for every heart beat.

3.4 Left Ventricle Work

For each simulation, the stroke work of the LV was determined. A bar plot has been made for comparison in figure 3.17.

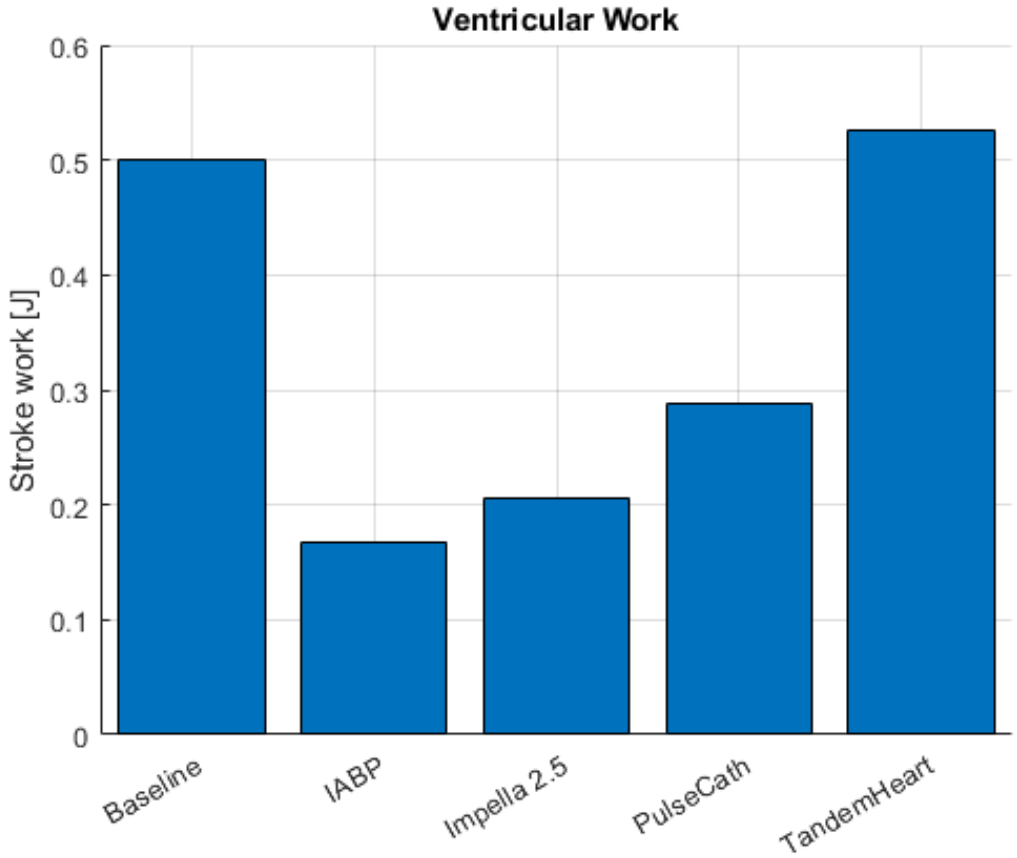

Figure 3.17: Work done by the left ventricle per simulation.

The baseline simulation shows a stroke work of 0.5 J. The TandemHeart shows a similar value. All other devices seem to lower the stroke work done by the LV. The ratios of LV work with MCS to baseline LV work are shown in table 3.2.

	Ratio of work done by LV
IABP	0.34
Impella 2.5	0.41
PulseCath	0.58
TandemHeart	1.05

Table 3.2: Work done by the left ventricle for each MCS device, relative to the baseline.

Chapter 4

Discussion

4.1 Lumped Parameter Study: Discussion of Methods

4.1.1 Model Accuracy

This study used the lumped parameter model of *Schampaert et al. (2011)* to evaluate various MCS devices in CS patients. Lumped parameter models are, by their definition, models that only calculate systemic values at their assigned nodal points. Modelling with a lumped parameter model that uses too few nodes would therefore result in inaccurate results. The model of *Schampaert et al.* should thus be discussed in this regard. The model consists of a total of 50 original nodes and 52 nodes for MCS simulation. Bifurcations of the system led through the myocard, head, abdomen, kidneys and legs. Arteries and veins were segmented into multiple systemic parts. The lungs were simulated with multiple Windkessel models. Though systems like these could always be more elaborate, it was considered adequate for the regard of MCS evaluation. The reason for this depends on the individual devices. MCS devices with pumping functions from the LV to the first aortic nodal point, are only passing the AV and do not require additional nodal points. Accurate afterload still depends on bifurcations and nodes, but this could still well be described with the used model [48].

A single fibre model was used to simulate heart beats, based on the work by *Bovendeerd et al. (2006)* This model assumed homogeneous fibre distribution over the ventricle, all represented by a single fibre. Though fibre distribution was well represented by this model, it could still be discussed whether assumptions of a single, homogeneously distributed fibre is a realistic representation. Still, *Bovendeerd et al. (2006)* showed realistic results in their study, meaning that implementation of the single fibre model in this study would be deemed appropriate.

4.1.2 Baseline Simulation

The baseline that was used in this study, represented a patient with CS. This was done by changing the parameters of the heart in the single fibre model. Parameters that were changed, were the contractility (from 1 to 0.4) and wall volume (from 200 ml to 150 ml) of the left heart and the contractility (from 1 to 0.8) of the right heart. This lowers heart performance, since the single fibre contracts with a lower maximum stress. Furthermore, the fibre volume is lowered, eventually resulting in lower stress of the ventricle wall. However, in reality, the ventricle wall is damaged at a specific region. This damaged region is barely able to contract,

if able to contract at all, whereas the rest of the ventricle contains healthy wall tissue, which tries to compensate for the loss of contractility. Even though *Bovendeerd et al. (2006)* proved that their model of the ventricle wall showed realistic performance for healthy heart tissue.

The single fibre model might not be able to model mechanical heart properties altered by anatomical changes, as a result of CS. Logically, it would have been preferred to have this more realistic behaviour included in the contraction model. However, the focus of this study lied on the simulation of time-dependent pressures and flows. The contraction of the single fibre model showed realistic change in pressure and volume in both ventricles, as their PV-loops have shown. Therefore, the single fibre model was considered to be realistic enough for this model study.

Another limitation to lumped parameter model in this study, is the static values of the present elements. When a patient is suffering from CS, blood pressure drops as a result of lowered heart performance. The body compensates for this loss of arterial pressure with vasoconstriction. The model does not include vasoconstriction. In order to accurately simulate CS, this could be implemented. However, implementation of vasoconstriction makes a more difficult comparison of MCS devices, since differences in flows and pressure would be influenced.

Furthermore, the baseline had a mean flow of 2.7 l/min with a MAP of 52 mmHg. Criteria for the definition of CS vary in literature [5]. The criteria in this study were based on the criteria by *Nativi et al. (2014)*, but may still not meet other criteria due to this varying definition [51]. Baseline results did show realistic CS patient values, but it is worth noting that comparison of this baseline with other studies might be more difficult, since baseline simulation results of a CS patient may consequently vary in these other studies.

4.1.3 Comparison of Healthy and Baseline Simulations

Using parameter values as determined by *Schampaert et al. (2011)*, a healthy person was simulated. This simulation had an output of 5.7 l/min and a MAP of 106 mmHg, which is in accordance with literature [54], though relatively high. The maximum systolic LV and aortic pressures were 130 mmHg, which is also relatively high, but still within expected values for healthy persons. As expected, the baseline shows lower pressure values of the LV, RV, aorta and pulmonary artery. Furthermore, the pressure in the LA is higher for the baseline, since the LV has too little power to pump blood coming from the pulmonary system, which is pumped there by the still relatively well functioning RV.

A curious result is shown in the comparison of the RV PV-loops in figure 2.4. For both simulations, the pressure is 0 mmHg during the filling phase. This is a result of an implementation, which does not allow the calculated ventricular pressure to drop below zero. The maximum systolic RV pressure is higher than expected, with a value of 40 mmHg. This is partly a result of a high LA pressure, which is approximately 11 mmHg, instead of an expected 5 mmHg [54]. This gives reason to doubt the realism of the simulation for the pulmonary system. However, values for both the LV and its afterload are as expected and are therefore considered reliable for this simulation.

4.1.4 Device Implementation

All devices, with the exception of the IABP, were implemented through two additional nodes, connecting the device with the inlet and outlet via resistances. These resistances increased

systemic stability. This implementation is certainly not ideal, since, even though calculations are stable, pumps with higher flow can still show oscillation. An example is shown in figure 6.1 in the appendix, where the pressures of a failed attempt of the Impella 5.0 implementation are shown. This oscillation is a result of the sudden change in volume in the system. Since volume is changed in the inlet node and outlet node, the pressure suddenly changes as well. This change in pressure causes a different flow in the next time step, which in turn gives a different change in pressure between these two nodes. These oscillating pressures may also cause flow through valves that would normally be closed, since pressure in e.g. the LV could momentarily be lower than in the AV. Therefore, not only pressures are unreliable, but flows as well.

A better implementation to this problem would be to have MCS devices change pressure, not volume or flow. Implementation of this was attempted by adding a negative resistance between these two nodes, and setting the value of this resistance as:

$$R_{MCS} = \frac{\Delta P}{q}$$

With dP the difference in pressure between the inlet and outlet and q the corresponding flow to that pressure difference. Unfortunately, this caused mathematical errors, leading to false solutions. For the devices that were observed in this study, the implementation that was used, showed no significant oscillation and was therefore accepted, but it should be noted that this solution, albeit an acceptable solution for these MCS devices, may not be acceptable for others.

4.1.5 Specific Device Limitations

IABP

The IABP was implemented by adding pressure nodes to the segments of the aorta, through a compliance. These pressure nodes varied in pressure from -200 mmHg to 200 mmHg, with a transition period of 0.135 s, in order to simulate IABP deflation and inflation. The compliance was related to the volume of the balloon. However, since IABP inflation and deflation time is dependent on aortic properties, values remain an estimation. Furthermore, as *Schampaert et al. (2011)* discussed, this device is sensitive to patient specific behaviour. This means that this device might show different results, for different patient parameters. This does not mean that results are not reliable though, since *Schampaert et al. (2011)* already proofed the model to be effective.

Impella 2.5

The Impella 2.5 simulated continuous, pressure-dependent flow from the LV to the aorta. This pressure dependency was based on the work by *Pennings et al. (2013)* on axial motors. This pressure dependency was created for a more realistic flow profile. Since *Pennings et al. (2013)* did not research the specific flow-differential-pressure relation in their study, this relation was based on that of the HeartMate II instead. Parameters were then altered, in order to meet literature flow values. For higher accuracy, the flow-differential-pressure relation of the Impella 2.5 could be researched. This study did not require said accuracy, since the simulated dependency was considered accurate enough. It could be worth investigating this

relation for simulations with high LV pressures (higher than 120 mmHg), but for patients with CS, these pressures are not reached.

PulseCath

The PulseCath that was simulated, was based on the iVAC 3L and had an output of 40 ml per cycle. This 40 ml was drawn from the LV during systole and ejected into the aorta during diastole. The flow of the PulseCath was not dependent on a pressure gradient, but was instead described as a half sine wave for both draw and ejection. In an in vivo situation, the PulseCath would be driven by an IABP driver, which makes flow pressure dependent. However, if it would be assumed that draw and ejection volume would always be the maximum amount of 40 ml, the only factor that would be important for describing outflow, is the flow profile. Instead of a half sine wave, other flow profiles could be chosen as well. For more accurate simulation, PulseCath flow profiles could be measured and evaluated. The importance of this is, however, still questionable, since literature has shown that different pump pulsatility profiles in rotary blood pumps have little effect on haemodynamics [55]. This gives reason to believe that the flow profile that describes the PulseCath inflow and outflow also gives little effect on the haemodynamics of these simulations, as long as this profile is pulsatile.

TandemHeart

The TandemHeart had inflow from the LA into the femoral artery and ha a pressure-dependent flow profile. Like the flow profile of the Impella 2.5, this flow profile was also based on the work by *Pennings et al. (2013)*, only based on centrifugal pumps instead of axial pumps. Instead of determining characteristic flow parameters by experimental measurement, these parameters were based on estimation. Like the estimation for the Impella, this estimation might be less accurate than actual measurements, but were considered accurate enough for these simulations, especially since the pressure difference between the LA and femoral artery has less fluctuation.

4.2 Lumped Parameter Study: Discussion of Results

4.2.1 Perfusion

All device simulations show a higher flow and MAP, compared to the baseline. This means that all devices contribute to perfusion of the system. However, devices with haemodynamic inflow and outflow cause the system to generate less flow through the AV, meaning that these devices mostly take over heart function, instead of giving support additionally.

The PP was also discussed. It shows that the baseline and IABP simulations have the highest PP, compared to other simulations. usage of an IABP would, due to its pulsatile behaviour, lead to more fluctuation in arterial pressure, as is seen in the results. Still, PP does not change under influence of the IABP. The PulseCath, which also creates a pulsatile flow, has a lower PP, since the minimal aortic pressure is higher, compared to the baseline simulation. This is as expected, since the PulseCath has outflow during diastole, resulting in a higher aortic pressure. Both the Impella and TandemHeart cause the minimal arterial pressure to rise as well, resulting in a lower PP. This is also as expected, since the continuous pump speed of both devices would logically result in a more continuous afterload.

4.2.2 MCS Device Flow

With the exception of the IABP, the devices used in this study have flow rates. These values have been examined. Results seem to show a correlation between a higher device flow and lower AV flow, combined with a higher mean flow. This conclusion can, however, not be drawn from these results alone, since these show flow in three different situations. A better way to evaluate this, would be to evaluate device flow and AV flow with the same pump with multiple RPM settings. In vivo studies have shown that these devices would contribute to LV unloading [56] and would thus lead to a lower cardiac output done by the heart itself. This gives reason to believe that a higher device flow would indeed lead to a lower AV flow in simulation studies.

The mean device flow is highest for the TandemHeart. This can be explained by the higher pressure-dependent flow rate the TandemHeart has. However, since the pressure of the LA was relatively high, as was discussed above, the TandemHeart most likely had a lower pressure-gradient over the inflow and outflow node. This influences flow rates and therefore also contributes to higher mean flow through the system.

Time-dependent flow was also evaluated. The highly continuous flow through the TandemHeart may be caused by the small changes in pressure-gradient. However, according to literature, PP in the femoral artery is approximately 17 mmHg [57]. Still, PP is a result of the pulsatile output of the LV. CS patients with a TandemHeart implanted, will have a lower arterial PP, compared to a baseline situation (34 mmHg vs 14 mmHg) [58]. This would explain the lowered femoral artery PP, resulting in an almost constant flow though the TandemHeart.

The PulseCath shows the expected half-sine, as a result of the prescribed inflow-outflow function. Inflow into the PulseCath is clearly the most pulsatile, compared to the other devices. This is also as expected because the other devices have a constant motor speed, whereas the PulseCath functions according to its pulsatile nature.

The Impella 2.5 shows a change in flow, despite constant motor speed. Since the pressure gradient between the LV and aorta changes throughout the heart cycle, this was expected. The difference between minimal flow and maximal flow is 1 l/min, with a mean flow of approximately 2.1 l/min. A proper function for pressure-dependent flow though the Impella was therefore considered important. As said earlier, the estimated parameters are considered accurate for this study, but since Impella flow evidently fluctuates, proper determination of this function might be essential in other studies.

4.2.3 Mechanical Work

Theoretically, the systemic energy and LV work done, should be equal. However a difference of 5% was found. Since the pressures of the LV were averaged by their previous time steps in the evaluated results, a minor inaccuracy of the calculated LV work is possible and would explain this difference. Furthermore, an inaccuracy of 5% was considered too low to be significant. It should however be noted, that this inaccuracy might be higher for the MCS implemented simulations.

As expected, implemented MCS devices lower the mechanical work done by the LV, both in absolute values and relative to the systemic uptake. An exception to this, is the IABP, which shows a higher LV work, compared to the baseline simulation. This still does not necessarily have a negative impact on the LV, since the IABP will increase coronary perfusion, which is

important for patients with CS [59].

Differences between the Impella and PulseCath exist as well. The PulseCath gives a higher systemic energy uptake, but a higher LV work done, compared to the Impella. A possible explanation is the fact that the Impella pumps during the systole, effectively lowering the LV volume, resulting in a lower value of $\int PdV$. However, the pulsatile nature of the PulseCath would, for the same reasons as the IABP, give a higher coronary perfusion.

The TandemHeart gives highest systemic energy uptake. A logical explanation would be the complete bypass of the LV, resulting in a lower SV, as is shown in the PV-loops. Since the TandemHeart has the highest device flow, it is understandable that the systemic energy uptake is higher, even with lower LV work.

4.3 Mock-loop Study: Discussion of Methods

4.3.1 Model Accuracy

The mock-loop model that was used in this study simulated the cardiovascular system. During each simulation, a different MCS device was evaluated. In contrast to the human cardiovascular system, this model simulated cardiovascular properties with resistances and compliances at specific points, rather than having this implemented continuously. This mock-loop did not include branches of the peripheral system and was instead modelled as a single systemic afterload. Furthermore, the atria that were modelled, did not contract and were instead modelled as compliance chambers, though contraction of the atria does occur in physiology. Since the mass that is present in the system, is dependent on the volume that was added, the amount differed from a physiological example. Still, if it is acceptable that this system only models specific parts of the cardiovascular system, resistances and compliances of the afterload could be adjusted accordingly, resulting in physiological or pathological flow and pressure behaviour. Since this study focused on the effects of MCS on heart properties and general perfusion, this limitation was considered acceptable. However, in retrospect, it would have been better to include the coronary system in this model, since the evaluated devices have different effects on coronary perfusion. This would be important to investigate in cases where CS patients are simulated.

The piston pumps that simulated ventricular behaviour, used servo motors to determine piston positions during the simulations. Though this meant that volume values of the ventricles could be determined and adjusted, the geometry and material properties of what would be the ventricle wall, are not accurate. This model would instead focus on the accurate simulation of volume change. Due to the restrictions in geometry, actual volumes that were present, were not in accordance with physiology. This resulted in a different latency in flow through the heart valves, since a different amount of mass needed to be accelerated. Furthermore, since the geometry of the used systems, were not according to the actual anatomy, MCS with devices based on this anatomy are not able to be implemented. Since the devices used in this study did not assume geometric ventricle properties, this was not a specific limitation. Still, future studies might need to evaluate this aspect for reliable results.

4.3.2 Baseline Simulation

The baseline experiment simulated a CS patient by using heart properties that would be valid for this pathology. As was done for the lumped parameter simulation, the parameters of the single fibre model were changed.

It was originally intended to use the same parameters for the lumped parameter model and the mock-loop model, but since these values did not successfully describe CS, parameters for the single fibre model were changed accordingly. This means that the values that were used for these parameters might not be accurate themselves, but since the pressure and volume characteristics of the LV were considered more important, this was acceptable.

As was stated for the lumped parameter model, the single fibre model might not be able to model mechanical heart properties with anatomical changes caused by CS. This unfortunately also applies for the mock-loop experiment. Originally, heart contraction was meant to be controlled by a time-varying elastance model. However, since this model led to systemic instabilities in practice, the single fibre model was used as an alternative.

The baseline was created according to literature values [51], stating that the peak systolic pressure should be below 90 mmHg. The mean flow was 3.1 l/min. However, since literature values differ, as was stated earlier, the baseline that was created here, may not be correct, according to every definition.

Furthermore, when the baseline was simulated, a certain resistance was applied. When MCS was switched on, this resistance did not change, to maintain reproducibility. In a clinical case, the arterial resistance would likely change, since this is subjected to altered vasoconstriction, caused by differences in perfusion.

Lastly, the behaviour of the RV was not reported mock-loop study. A known limitation to this system, is the incapability to properly model this behaviour of the RV. For example, PV-loops do not show isovolumetric contraction and relaxation. However, peak systolic RV pressure was around 30 mmHg, which was considered adequate, based on literature values [54]. Though a more realistic representation of the RV would always be desired, the main focus was the modelling of the LV, since this is the main point of interest when CS is treated.

4.3.3 Specific Device Limitations

IABP

The IABP was inserted through an inlet inside a tapered resistance screw, distal from the aorta. In contrast to a physiological example, the aorta that was used in this mock-loop study had no bifurcations. In a physiological situation, the IABP would cause the blood in the aortic arch to flow into the present branches and therefore only partially causing flow further distal into the aorta. Positioning of the IABP would therefore be of importance. Since the aorta neither contained these side branches, nor had the geometrical properties of the aorta, these effects could not be studied. These effects could, however, be of influence on the perfusion of both specific arteries and perfusion in general.

4.3.4 Impella 2.5

The Impella 2.5 was meant to be controlled with the Impella driver, which is also used in the clinic. The driver was supposed to give level P7 support, resulting in a motor revolution speed of 47000 RPM [60]. Since this device was not available, the Impella 2.5 was controlled with non-standard equipment. This equipment controlled the Impella instead, still with a revolution speed of 47000 RPM. Furthermore, during earlier experiments, measurements with the Impella were attempted with a silicone rubber valve. Since the Impella caused regurgitation, the silicone rubber valve was replaced with a porcine AV. Since this valve needed to be kept in its solution, a minimum duration of usage was desired. Therefore this valve was only used during the Impella and PulseCath experiments. Using this valve, instead of the silicon rubber valve, could have influenced the acquired results.

4.3.5 PulseCath

The PulseCath iVAC 3l was inserted through a, normally closed, side branch of the aorta. The PulseCath was then inserted into the LV, through the porcine AV. The outlet valve of the PulseCath had an oscillation during outflow into the aorta. This oscillation influenced measurements of the aortic pressure, since this caused a pressure wave. During the evaluated

results, this oscillation did not occur. It was assumed that this influence earlier, did not cause any significant effect during the evaluated time.

4.3.6 TandemHeart

The TandemHeart was connected by two silicone rubber tubes. One tube was inserted into the LA compliance tank, while the other tube was inserted into the distal part of the aorta. Initially, the experiment meant to include a TandemHeart driver. Since this driver was not available, the same set-up was used as for the Impella. This set-up controlled the TandemHeart at 7500 RPM. Normally, the TandemHeart outlet tube would be inserted into the femoral artery, but since the aorta that was used, was directly connected to the systemic afterload, a simplified set-up was used. Placement of this outlet tube could therefore have influenced pressure and flow results that were evaluated.

4.4 Mock-loop Study: Discussion of Results

4.4.1 Perfusion

The baseline that was simulated, had a flow of 3.1 l/min and a MAP of 54 mmHg. It was expected that these four MCS options would raise both mean flow and MAP. However, the IABP and PulseCath did not significantly raise these values. Still, the SV and peak systolic LV pressure were significantly lower, compared to the baseline. This would explain the difference in both mean flow and MAP. It also shows that these devices take over heart function in these simulations.

The aortic pressures that were discussed, showed different curves. The PulseCath had a more continuous pressure profile, since this device ejects during the diastole, thereby lowering the PP. Impella lowers LV SV, which in turn lowers the PP. The TandemHeart showed a similar curve compared to the baseline, only higher in pressure values. This can be explained by the little influence the TandemHeart had on the SV and pressure of the LV. It was expected though, that the TandemHeart would have lowered the SV of the LV, by drawing volume from the LA, and bypassing the LV completely, but this is not shown in this experiment. However, literature would suggest that the TandemHeart would lower the SV of the LV [61]. The IABP has the highest PP, which was as expected. Still the minimal pressure in the aorta was 0 mmHg. Since this would be the atmospheric pressure, this may very likely not be accurate. A disturbance in this curve is shown at a pressure of 80 mmHg. This disturbance is caused by a pressure wave reflection at the point where the aorta is connected at the systemic afterload. The systemic afterload could be designed in a different way, in order to prevent this, but this study accepted this inaccuracy instead.

4.4.2 TandemHeart Flow

This study wanted to measure flow through each individual device. Because there was no suitable flow meter to measure flow through the PulseCath and Impella, this was not possible. However, since the TandemHeart used tubes that were outside of the experimental set-up, it was possible to include a flow meter. Flow that was measured through the TandemHeart, varied between 0.6 l/min during end-systole and 1.3 l/min during end-diastole. The mean flow was 1 l/min. This was lower than expected, since the TandemHeart should be able to

pump up to 4 l/min at a speed of 7500 RPM [62]. This may be caused by the difference in viscosity between blood and water. A more continuous flow profile was also expected, but because of this lower mean flow, the LV would be more active. This would give more pulsatility compared to the expected situation.

4.4.3 Mechanical Work

Originally, this study was to include the systemic uptake in terms of energy in the results. This uptake would have been calculated as:

$$E_{system} = d\hat{P} \cdot \hat{q} \cdot t$$

The values of these results were, however, a factor 2 lower than the LV work done and were therefore considered unreliable. It would be beneficial to know these values, since these would clarify both the energy uptake by the system and the work done by the used MCS devices. It should also be noted, that the pressure values of the shown PV-loops contain negative values, meaning that the LV pressure values are below atmospheric pressure. This means that the pressure signals were most likely not correctly calibrated. Since no reasonable compensation could be applied, this was accepted as a limitation.

The work done by the LV could still be calculated. With the exception of the TandemHeart, all devices lowered the mechanical LV work, though the TandemHeart was the only MCS device that contributed to the perfusion. However, since the PV-loop that was found, did not show the results as were expected in literature, the calculated work that was based on this PV-loop, is questionable. The Impella, however, showed a PV-loop that was according to literature values [61]. The work that was calculated from this, was therefore considered reliable. The found work was 0.2 J, which is only 40% of the energy done by the LV in the baseline simulation.

According to the same literature, the PulseCath should have a similar effect as the Impella on the PV-loop. Differences between these loops were the isovolumetric relaxation and higher SV. This was considered valid, since the PulseCath does not draw volume during the diastole, resulting in less volume draw and no change of volume during the beginning of the diastole. The LV had a work of 0.3 J, meaning that the PulseCath effectively lowers the LV work.

The PV-loop taken from the IABP support simulation shows a peak systolic LV pressure of 40 mmHg, which is a factor 2 lower than the baseline simulation. The PV-loop also shows a significant volume shift to the left, compared to the baseline. However, according to literature values, there should be no effective change in the PV-loop of the LV [63]. Differences in there results may be caused by the difference in LV afterload, caused by the IABP, since the IABP in this study lowered the aortic pressure considerably. Results for this simulation are therefore questionable, since it was already pointed out that the aortic pressure with IABP support may not be reliable.

4.5 Comparison of the Lumped Parameter Model and Mock-Loop Model

4.5.1 Systemic Differences

Several differences existed between the two used models. The lumped parameter model had 50 different nodes, which were used for pressure and flow calculations. The arteries also branched into multiple peripheral systems. The mock-loop model, however, did not have these branches, nor these many different sections of the cardiovascular system. This might have led to different results in both models. Furthermore, the fact that the lumped parameter model is software from which pressures and flows can be saved and read at any given node in the system, research of this software model is done relatively easy. For hardware models, such as the mock-loop model, research usually include a change or adaptation of existing hardware. This would logically be less convenient than changing software settings.

Aside from branching and nodal points, the mock-loop model had some physical limitations, compared to the lumped parameter model. First of all, the systemic afterload models that were used, consisted of compliance tanks and tapered resistance screws. The compliances and resistances that were set, were iteratively set according to the pressure and flow results that were found in the aorta. Although markings were used, these compliances and resistances showed to be sensitive to small changes, therefore making it hard to stay at the exact same values. This is, of course, different for software models with only numerical input.

Another limitation to the mock-loop model, was the inability to realistically represent the ventricle volumes and connections to the valves. The ventricle compartments consisted of hard material, which did not represent the ventricles geometrically. Leading to a difference in latency and compliance. For the lumped parameter model, however, these values could be set as input, meaning that the ventricular properties could be represented better in this regard.

4.5.2 Differences in Results

Baselines

Since the lumped parameter model has the same baseline for every MCS simulation, no differences in baseline simulations exist. This is not true for the mock-loop study, since these baselines needed to be measured for each MCS simulation. These baselines did show differences, meaning that the MCS measurements were influenced by different baselines. These baselines were considered similar and differences were therefore disregarded, but exact situations like the simulation of the lumped parameter model, would logically be better for reproducibility and comparison.

PV-Loops

The PV-loops that were observed in both models, had different outcomes. First of all, the baseline that was found in the lumped parameter study, had higher volumes compared to the mock-loop study (118 ml - 153 ml and 37 ml- 74 ml respectively). Differences could have been caused by different parameter values in the single fibre model. When MCS is applied, the PV-loops acquired from the lumped parameter study show less drop in peak systolic pressure, compared to the mock-loop study. The IABP and TandemHeart seemed to show different

results, compared to literature, in the mock-loop study, whereas the lumped parameter study showed results accordingly.

Aortic Pressure and Pulse Pressure

The aortic pressures that were acquired for the TandemHeart, similar MAP but different PP results. PP results would perhaps be similar, if the mean flow through the TandemHeart would be the same in these two simulations, but this has not been researched.

The Impella shows lower PP in both situations, but a lower MAP in the mock-loop study. Literature shows that MCS of the Impella 2.5 should lead to higher MAP [64], which gives reason to believe that the lumped parameter model gives more realistic results in this situation.

The PulseCath also shows a lower PP in both situation but a lower MAP in the mock-loop study. In this case, literature also suggests that the PulseCath should give a higher MAP [35] and would therefore give reason to believe that the lumped parameter model gives more realistic results in this situation as well.

The IABP has a similar effect on both the mock-loop study and lumped parameter model, but has a PP of 130 mmHg in the mock-loop study compared to a PP of 22 mmHg in the lumped parameter study. This difference is caused by the extreme drop in aortic pressure in the mock-loop study. When literature findings of experiments with the IABP are reviewed, the results of the lumped parameter study are more comparable and therefore considered more realistic [65].

Data of Work and Energy

The results of Work done in the LV in the mock-loop study, gave values for MCS relative to the baseline, compared to the lumped parameter model. This is caused by the different effects these devices have on the PV-loops. The discussion of these PV-loops drew the conclusion that the results of the lumped parameter model are more realistic in this regard. Since the calculations of the LV work are based directly on the data of these PV-loops, the calculated LV work is therefore considered more realistic in the lumped parameter study as well.

Chapter 5

Conclusions

This study attempted to compare four MCS devices in both a simulated lumped parameter model and a mock-loop model. The performance of these devices were evaluated based on their influences on mean flow, arterial pressure, LV volumes and pressures and flow through MCS devices. According to the lumped parameter model, the TandemHeart gives the highest improvement in perfusion, while reducing LV work. The PulseCath iVAC 3l and Impella 2.5 give show less performance in perfusion and LV work reduction compared to the TandemHeart and show similar results in these regards compared to each other. The IABP has little improvement on perfusion and LV work reduction, but does show a high, PP with respect to the other MCS devices.

The mock-loop model Showed contradicting results. The TandemHeart does have the highest effect on perfusion, but does not lower LV work. In addition, the LV work with IABP support is lowered to 33% of the baseline LV work. The Impella and PulseCath do improve flow, but do not improve MAP. The IABP did show improvement of PP. Other devices showed lower PP during MCS.

Comparison of these models showed that the lumped parameter study gave more accurate values, according to found literature. Therefore, the lumped parameter model would give a better comparison of the simulated MCS devices that were used in this study, compared to the mock-loop model. This in turn gives reason to believe, that the lumped parameter model may give more accurate results on other MCS devices as well. Still, the MCS devices that were implemented in the lumped parameter model, were simulated, either based on experimental data of these devices themselves, or derived from experimental data similar to these devices. Unless characteristics of a different MCS device can be estimated without experimental data, it would not be possible to simulate such a device. It is therefore likely that a prototype of a new MCS device cannot directly be tested with a lumped parameter study and would require experimental data from e.g. animal test or mock-loop studies instead.

The used mock-loop study at the TU/e showed questionable results regarding MCS flow, arterial pressure and LV behaviour. New prototypes could always be observed in this experimental set-up, but conclusions from such experiments should be drawn carefully. These prototypes could instead be tested with animal test studies, but this would unfortunately include the disadvantages that animal tests have. Mock-loop experiments may therefore still be desirable, but in order to test MCS with the used mock-loop reliably, the discussed points in this study need to be implemented. Only then can mock-loop experiments be the preferred option for testing MCS.

Bibliography

[1] World health Organization. Who methods and data sources for life tables 1990-2016, march 2018. `http://apps.who.int/gho/data/view.main.SDG2016LEXREGv?lang=en`, Last accessed on 2019-04-11.

[2] World health Organization. Global health estimates 2016 summary tables: Deaths by cause, age and sex, by world bank income group, 2000-2015, April 2018. `https://www.who.int/healthinfo/global_burden_disease/GHE2016_Deaths_WBInc_2000_2016.xls`, Last accessed on 2019-04-11.

[3] Y. Pinto. Three decades of heart transplantation in the netherlands. *Netherlands Heart Journal*, 25(9):469–470, September 2017.

[4] L. Ajello A. Sansone M. Caruso Pasquale Assennato E. La Franca, R. Iacona. Heart failure and mechanical circulatory assist devices. *Global Journal of Health Science*, 5(5):11–19, April 2013.

[5] C. Vahdatpour, D. Collins, and S. Goldberg. Cardiogenic shock. *Journal of the American Heart Association*, 8(8):1–12, April 2019.

[6] S. van Diepen, J. Katz, N. Albert, T. Henry, A. Jacobs, N. Kapur, A. Kilic, V. Menon, M. Ohman, N. Sweitzer, H. Thiele, J. Washam, and M. Cohen. Contemporary management of cardiogenic shock: A scientific statement from the american heart association. *Circulation*, 136(16):232–268, 2017.

[7] J. Hochman, L. Sleeper, J. Webb, T. Sanborn, H. White, D. Talley, C. Buller, A. Jacobs, J. Slater, J. Col, S. McKinlay, M. Picard, M. Menegus, J. Boland, V. Dzavik, C Thompson, C. Wong, R. Steingart, R. Forman, P. Aylward, E. Godfrey, P. Desvigne-Nickens, and T. LeJemtel. Early revascularization in acute myocardial infarction complicated by cardiogenic shock. *New England Journal of Medicine*, 341(9):625–634, August 1999.

[8] M. Patel, R. Smalling, H. Thiele, H. Barnhart, Y. Zhou, P. Chandra, D. Chew, M. Cohen, J. French, D. Perera, and M. Ohman. Intra-aortic balloon counterpulsation and infarct size in patients with acute anterior myocardial infarction without shock: The crisp ami randomized trial. *JAMA*, 306(12):1329–1337, September 2011.

[9] A. Berkefeld M. Krane R. Lange B. Voss A. Prinzing, U. Herold. Left ventricular assist devices current state and perspectives. *Journal of Thoracic Disease*, 8(8), August 2016.

[10] ED. Liotta. Early clinical application of assisted circulation. *Texas Heart Institute, Houston*, 29(3):229–230, 2002.

[11] J. Hassoulas J. Brink. The first human heart transplant and further advances in cardiac transplantation at groote schuur hospital and the university of cape town. *Cardiovascular Journal of Africa*, 20(1):31–35, February 2009.

[12] L. Loza B. Bruckner J. Estep, B. Trachtenberg. Continuous flow left ventricular assist devices: Shared care goals of monitoring and treating patients. *Methodist Debakey Cardiovascular journal 2015*, 11(1):33–44, March 2015.

[13] P. Baer J. Frank W. Lemm F. Zartnack E. Bticherl, E. Hennig. Status of the artificial heart program in berlin. *Societe Internationale de Chirurgie*, 9(1):103–115, 1985.

[14] N. Stolf. History of heart transplantation: a hard and glorious journey. *Brazilian Journal of Cardiovascular Surgery*, 329(5):423427, September 2017.

[15] G. Hallman R. Bloodwell R. Leachman J. Milam D. Cooley, D. Liotta. Orthotopic cardiac prosthesis for two-staged cardiac replacement. *The American Journal of Cardiology*, 24(5):723–730, November 1969.

[16] A. Dipchand S. Goldfarb A. Kucheryavaya B. Levvey B. Meiser J. Rossano R. Yusen J. Stehlik L. Lund, L. Edwards. The registry of the international society for heart and lung transplantation: Thirty-third adult heart transplantation report2016; focus theme: Primary diagnostic indications for transplant. *The Journal of Heart and Lung Transplantation*, 35(10):1158–1169, October 2016.

[17] W. Bernhard D. Pennington C. Haudenschild N. Ratliff R. Berger L. Golding J. Watson F. Schoen, D. Palmer. Clinical temporary ventricular assist. pathologic findings and their implications in a multi-institutional study of 41 patients. *he Journal of Thoracic and cardiovascular Surgery*, 92(6):1071, December 1986.

[18] A. Berson. Ventricular assist systems for temporary life support: Device readiness testing. *IEEE Engineering in Medicine and Biology Magazine*, 7(2):92–93, June 1988.

[19] M. Bergheim R. Delgado. Heartmate ii left ventricular assist device: a new device for advanced heart failure. *Expert Review of Medical Devices*, 2(5):529–532, January 2005.

[20] T. Aizawa M. Shiono I. Sakuma S. Takatani J. Glueck G. Noon Y. Nos M. DeBakey T. Sasaki, T. Jikuya. A compact centrifugal pump for cardiopulmonary bypass. *Artificial Organs*, 16(6):592–598, December 1992.

[21] L. McBride, K. Naunheim, A. Fiore, D. Moroney, and M. Swartz. Clinical experience with 111 thoratec ventricular assist devices. *The Annals of Thoracic Surgery*, 67(5):1233–1238, May 1999.

[22] M. Boucek B. Trulock M. Deng B. Keck M. Hertz D. Taylor, L. Edwards. Registry of the international society for heart and lung transplantation: Twenty-second official adult heart transplant report2005. *The Journal of Heart and Lung Transplantation*, 24(8):945–955, August 2005.

[23] E. Rose, A. Gelijns, A. Moskowitz, D. Heitjan, L Stevenson, W. Dembitsky, J. Long, D. Ascheim, A. Tierney, R. Levitan, J. Watson, N. Ronan, P. Shapiro, R. Lazar, L. Miller, L. Gupta, H. Frazier, P. Desvigne-Nickens, M. Oz, V. Poirier, and P. Meier. Long-term

use of a left ventricular assist device for end-stage heart failure. *New England Journal of Medicine*, 345(20):1435–1443, November 2001.

[24] K. Lietz, J. Long, A. Kfoury, M. Slaughter, M. Silver, C. Milano, J. Rogers, Y. Naka, D. Mancini, and L. Miller. Outcomes of left ventricular assist device implantation as destination therapy in the post-rematch era. *Circulation*, 116(5):497–505, July 2007.

[25] V. Venugopal. A novel technique for intra-aortic balloon positioning in the intensive care unit. *Journal of ExtraCorporeal Technology*, 44(3):160–162, September 2012.

[26] NMC Heartcare. Iabp (intra-aortic balloon pump) insertion.

[27] S. Moulopoulos, S. Topaz, and W. Kolff. Diastolic balloon pumping (with carbon dioxide) in the aorta–a mechanical assistance to the failing circulation. *American Heart Journal*, 63(5):669–675, May 1962.

[28] H. Parissis, V. Graham, S. Lampridis, M. Lau, G. Hooks, and P. C. Mhandu. Iabp: history-evolution-pathophysiology-indications: what we need to know. *Journal of Cardiothorac Surgery*, 11(1):122, August 2016.

[29] D. Brown. *Cardiac Intensive Care (Third Edition)*. Elsevier, Washington University School of Medicine, St. Louis, Missouri, October 2018.

[30] C. Davidsen, E. Packer, K. Lland, S. Rotevatn, E. Nygreen, E. Eriksen, A. ksnes, J. Herstad, R. Haaverstad, . Bleie, and V. Tuseth. Impella use in acute myocardial infarction complicated by cardiogenic shock and cardiac arrest: Analysis of 10 years registry data. *Resuscitation*, April 2019.

[31] O. Maniuc, T. Salinger, F. Anders, J. Mntze, D. Liu, K. Hu, G. Ertl, S. Frantz, and P. Nordbeck. Impella cp use in patients with nonischaemic cardiogenic shock. *ESC Heart Failure*, advanced publication, October 2018.

[32] E. Hong and T. Naseem. Color doppler artifact masking iatrogenic aortic valve injury related to an impella device. *Journal of Cardiothoracic and Vascular Anesthesia*, 33(6):1584–1587, June 2019.

[33] Y. Nakao, J. Aono, T. Tasaka, T. Uetani, H. Higashi, S. Ikeda, T. Yorozuya, H. Izutani, and O. Yamaguchi. Impella 5.0 mechanical assist device catheter-induced severe hemolysis due to giant swinging motion new concern in impella usage . *Circulation Journal*, advanced publication, March 2019.

[34] B. Wernly, C. Seelmaier, D. Leistner, B. Sthli, I. Pretsch, M. Lichtenauer, C. Jung, U. Hoppe, U. Landmesser, H. Thiele, and A. Lauten. Mechanical circulatory support with impella versus intra-aortic balloon pump or medical treatment in cardiogenic shocka critical appraisal of current data. *Clinical Research in Cardiology*, advanced publication, March 2019.

[35] C. den Uil, Daemen J, M. Lenzen, A. Maugenest, L. Joziasse, R. Geuns, and N. Van Mieghem. Pulsatile ivac 2l circulatory support in high-risk percutaneous coronary intervention. *EuroIntervention*, 12(14):1689–1696, February 2017.

[36] A. Amicoa, M. Brigianib, A. Vallabinia, B. Ferrantea, A. Marzovilloa, D. Loizzia, and C. Carbonea. Pulsecath, a new short-term ventricular assist device: our experience in off-pump coronary artery bypass graft surgery. *Circulation*, 9(4):423–426, May 2008.

[37] K. Anastasiadis, O. Chalvatzoulis, P. Antonitsis, P. Tossios, and C. Papakonstantinou. Left ventricular decompression during peripheral extracorporeal membrane oxygenation support with the use of the novel ivac pulsatile paracorporeal assist device. *The Annals of Thoracic Surgery*, 92(6):2257–2259, December 2011.

[38] N. van Mieghem, J. Daemen, M. Lenzen, R. Zandstra, O. Malkin, and R.J. van Geuns. The pulsecath ivac 2l left ventricular assist device: conversion to a percutaneous transfemoral approach. *Interventions for Hypertension and Heart Failure*, 11(7):835–839, November 2015.

[39] P. Vranckx, E. Meliga, P. de Jaegere, M. van den Ent, E. Regar, and P. Serruys. The tandemheart, percutaneous transseptal left ventricular assist device: a safeguard in high-risk percutaneous coronary interventions. the six-year rotterdam experience. *EuroIntervention*, 4(3):331–337, November 2008.

[40] A. Afzal and S. Hall. Percutaneous temporary circulatory support devices and their use as a bridge to decision during acute decompensation of advanced heart failure. *EuroIntervention*, 31(4):453–456, October 2018.

[41] M. Shishehbor, N. Moazami, M. Tong, S. Unai, W. Wilsong-Tang, and E. Soltesz. Cardiogenic shock: From ecmo to impella and beyond. *Cleveland Clinic Journal of Medicine*, 84(4):287–295, July 2017.

[42] Cardiac assist receives health canada approval for tandemheart circulatory support platform. https://www.dicardiology.com/content/cardiacassist-receives-health-canada-approval-tandemheart-circulatory-support-platform, April 2014.

[43] A. Alabbady, A. Abdul-Al, and K. Skelding. Left ventricular assisting devices in percutaneous coronary intervention. *US Cardiology Review*, 11(2):86–94, 2017.

[44] C. Nix and F. Menzler. From a lab type to a product: A retrospective view on impella's assist technology. *Artificial Organs*, 25(5):414–421, January 2002.

[45] H. Loree II, K. Bourque, D. Gernes, J. Richardson, V. Poirier, N. Barletta, A. Fleischli, G. Foiera, T. Gempp, R. Schoeb, K. Litwak, T. Akimoto, M. Kameneva, M. Watach, and P. Litwak. The heartmate iii: Design and in vivo studies of a maglev centrifugal left ventricular assist device. *Artificial Organs*, 25(5):386–391, January 2001.

[46] A. Stonehouse, M. Cook, and J. Woodard. Ventrassist left ventricular assist systems long-term in vitro reliability. *Artificial Organs*, 33(10):860–864, October 2009.

[47] P. Bovendeerd, P. Borsje, T. Arts, and F. van de Vosse. Dependence of intramyocardial pressure and coronary flow on ventricular loading and contractility: A model study. *Annals of Biomedical Engineering*, 34(12):18331845, December 2006.

[48] S. Schampaert, M. Rutten, M. van t Veer, L. van Nunen, P. Tonino, N. Pijls, and F. van de Vosse. Modeling the interaction between the intra-aortic balloon pump and

the cardiovascular system: The effect of timing. *Interactive CardioVascular and Thoracic Surgery*, 12(6):912913, June 2013.

[49] S. Schampaert, M. vant Veer, F. van de Vosse, N. Pijls, B. de Mol, and M. Rutten. In vitro comparison of support capabilities of intra-aortic balloon pump and impella 2.5 left percutaneous. *Artificial Organs*, 35(9):893901, August 2011.

[50] T. Arts, P. Bovendeerd, T. Delhaas, and F. Prinzen. Modeling the relation between cardiac pump function and myofiber mechanics. *Journal of Biomechanics*, 36(5):731736, June 2003.

[51] J. Nativi-Nicolaua, C. Selzmanc, J. Fanga, and J. Stehlika. Pharmacologic therapy for cardiogenic shock. *Current Opinion in Cardiology*, 29(4):250257, May 2014.

[52] Sandro Gelsomino, Attilio Renzulli, Antonino S. Rubino, Salvatore Mario Romano, Fabiana Luc, Serafina Valente, Gian Franco Gensini, and Roberto Lorusso. Effects of 1:1, 1:2 or 1:3 intra-aortic balloon counterpulsation/heart support on coronary haemodynamics and cardiac contractile efficiency in an animal model of myocardial ischaemia/reperfusion. *European Journal of Cardio-Thoracic Surgery*, 42(2):325–332, 02 2012.

[53] K. Pennings, J. Martina, B. Rodermans, J. Lahpor, F. van de Vosse, B. de Mol, and M. Rutten. Pump flow estimation from pressure head and power uptake for the heartassist5, heartmate ii, and heartware vads. *ASAIO Journal*, 59(4):420426, March 2013.

[54] R. Klabunde. *Cardiovascular Physiology concepts*. Philadelphia, PA : Lippincott Williams Wilkins/Wolters Kluwer. Wolters Kluwer Health, 2005. ISBN:978-1-4511-1384-6.

[55] T. Pirbodaghi, S. Axiak, A. Weber, T. Gempp, and S. VandenBerghe. Pulsatile control of rotary blood pumps: Does the modulationwaveform matter? *The Journal of Thoracic and Cardiovascular Surgery*, 144(4):970–977, October 2012.

[56] R. Asleh and J. Resar. Utilization of percutaneous mechanical circulatory support devices in cardiogenic shock complicating acute myocardial infarction and high-risk percutaneous coronary interventions. *Journal of Clinical Medicine*, 8(8):1–33, October 2019.

[57] A. Protogerou, T van Sloten, R. Henry, J. Dekker, G. Nijpels, and C. Stehouwer. Pulse pressure measured at the level of the femoral artery, but not at the level of the aorta, carotid and brachial arteries, is associated with the incidence of coronary heart disease events in a population with a high prevalence of type 2 diabetes and impaired glucose metabolisme - the hoorn study. *Artery Research*, 9:19–26, January 2015.

[58] B. Weil, F. Konecny, G. Suzuki, V. Iyer, and J. Canty. Comparative hemodynamic effects of contemporary percutaneous mechanical circulatory support devices in a porcine model of acute myocardial infarction. *JACC: Cardiovascular Interventions*, 9(22):2292–2303, November 2016.

[59] T. Aye, Z. Htet, T. Singhavilai, and P. Naiyanetr. Effect of intra-aortic balloon pump on coronary blood flow during different balloon cycles support a computer study. *JACC: Cardiovascular Interventions*, 11(4):3303–3306, August 2015.

[60] Abiomed. Impella2.5 with the automated impella controller circulatory support system, instructions for use clinical reference manual (united states only). Abiomed, Inc. 22 Cherry Hill Drive, Danvers, Massachusetts 01923 USA, Voice: 978-777-5410, Facsimile: 978-777-8411, Email: clinical@abiomed.com.

[61] D. Burkhoff, G. Sayer, and D. Doshi N. Uriel. Hemodynamics of mechanical circulatory support. *Journal of the American College of Cardiology*, 66(23):2663–2674, December 2015.

[62] B. Kar, L. Adkins, A. Civitello, P. Loyalka, N. Palanichamy, C. Gemmato, T. Myers, I. Gregoric, and R. Delgado. Clinical experience with the tandemheart percutaneous ventricular assist device. *Texas Heart Institute Journal*, 33(2):111–115, December 2006.

[63] O. Kawaguchi, W. Pae, B. Daily, and W. Pierce. Ventriculoarterial coupling with intra-aortic balloon pump in acute ischemic heart failure. *The Journal of Thoracic and Cardiovascular Surgery*, 117(1):164–171, January 1999.

[64] S. Dixon, J. Henriques, L. Mauri adn K. Sjauw, A. Civitello, B. Kar, P. Loyalka andF. Resnic, P. Teirstein, R. Makkar, I. Palacios andM. Collins, J. Moses, and K. Benali andW. ONeill. A prospective feasibility trial investigating the use of the impella 2.5 system in patients undergoing high-risk percutaneous coronary intervention (the protect i trial). *JACC: Cardiovascular Interventions*, 2(2):91–96, February 2009.

[65] C. Bartoli, B. Rogers, C. Ionan, and G. Pantalos. End-diastolic flow reversal limits the efficacy of pediatric intra-aortic balloon pump counterpulsation. *The Journal of Thoracic and Cardiovascular Surgery*, 147(5):1660 – 1667, May 2014.

Chapter 6

Appendix

6.1 Simulation Model

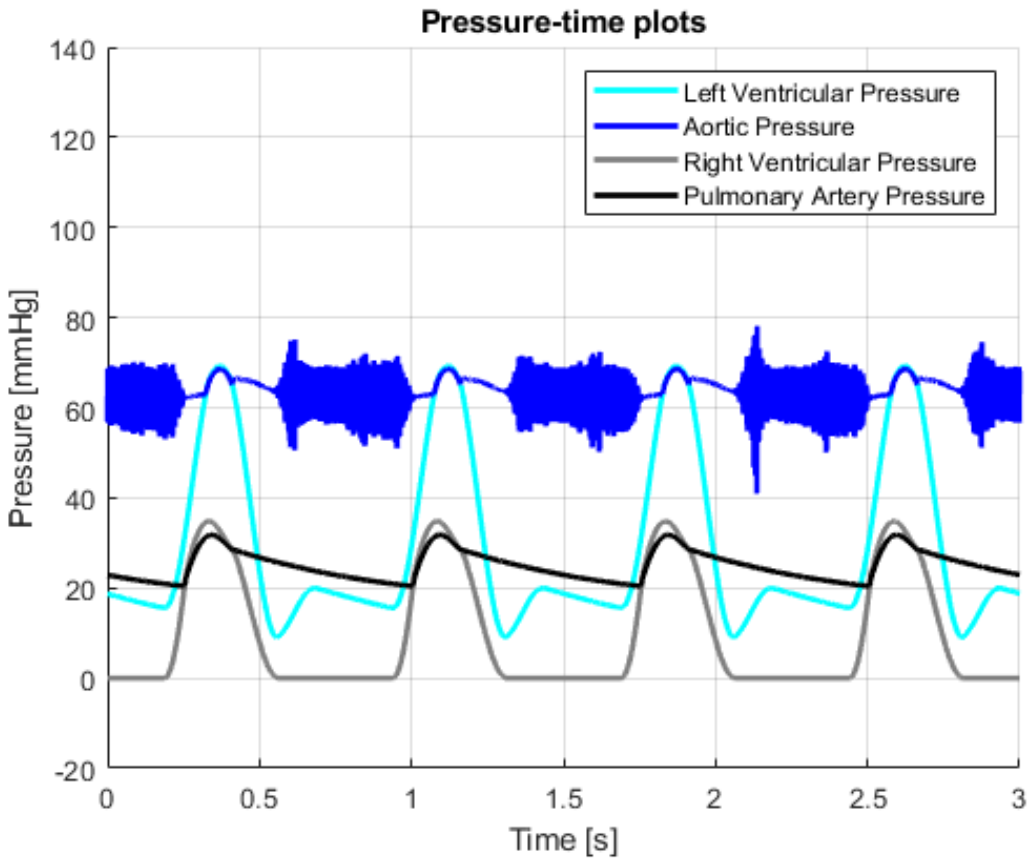

Figure 6.1: Pressure-time curves of the left ventricle, as well as the preload and afterload, for the Impella 5.0 simulation.

6.2 Mock-loop experiment Procedure

6.2.1 Device implementation

IABP Implementation

1. Place the IABP into the aorta, through the inlet distal from the aorta.
2. Connect the IABP to the driver.
3. Connect the driver to the PC.
4. Enable the IABP control in the system, with support ratio 1:1.

PulseCath Implementation

1. Place the PulseCath into the LV and the aorta, through the alternate LV inlet and separate, most proximal, branch on the aorta.
2. Connect the PulseCath to the IABP driver.
3. Connect the driver to the PC.
4. Enable the IABP control in the system, with support ratio 1:1.

Impella Implementation

1. Place the Impella into the LV and the aorta, through the alternate LV inlet and separate, most proximal, branch on the aorta.
2. Connect the Impella to the LVAD driver.
3. Connect the driver to the PC.
4. Enable the LVAD control in the system.

TandemHeart Implementation

1. Place the TandemHeart into the AV and the aorta, through the alternate AV inlet and separate, most distal, branch on the aorta.
2. Connect the Impella to the LVAD driver.
3. Connect the driver to the PC.
4. Enable the LVAD control in the system.

6.2.2 System preparation

1. Fill all compliances according to their indication marks.
2. Balance all pressure sensor amplifiers.
3. Apply a filling pressure of 7 mmHg.
4. Start a simulation with default settings.
5. Adjust resistances, until physiological pressure- and flow values are reached.
6. Stop the simulation.
7. Set the RV contractility to 0.8, the LV contractility to 0.4, the wall volume to $160 \cdot 10^{-2}$ m^3 and cavity volume to $60 \cdot 10^{-2}$ m^3 in the four_chamber_model.c script.
8. Recompile the c script. Rebuild the Matlab program.
9. Set the heart rate to a fixed value of 80 BPM in Simulink.

6.2.3 Initiating experiments

1. Start the mock-loop experiment after all necessary preparations are performed.
2. Wait for the system to reach a steady state.
3. Confirm if the steady state shows the expected pathological properties.
4. If this measurement is performed with a MCS device, initiate this device. Set the device performance to a maximum gradually.
5. When maximum performance is reached, confirm if the system is in a steady state.
6. Continue measurements in steady state for 30s.
7. Stop the experiment. All data will be saved to the file *fcm1.mat*.

6.3 Disclaimer: Requesting Matlab Simulation Code

Since the vast majority of the used code was written by others and is legally owned by the TU/e, the source code is not publicly available. Those who are interested in examining this code or want to use it, can request this code from Marcel Rutten at the TU/e.